Climate, demography, immunology, and virology combine to drive two decades of dengue virus dynamics in Cambodia

Cara E. Brook[1*], Carly Rozins[2], Jennifer A. Bohl[3], Vida Ahyong[4], Sophana Chea[5], Liz Fahsbender[6], Rekol Huy[7], Sreyngim Lay[5], Rithea Leang[7], Yimei Li[1], Chanthap Lon[5], Somnang Man[5,7], Mengheng Oum [5], Graham R. Northrup[8], Fabiano Oliveira[3], Andrea R. Pacheco[5], Daniel M. Parker[9,10], Katherine Young[11], Michael Boots[12], Cristina M. Tato[4], Joseph L. DeRisi[4], Christina Yek[3], Jessica E. Manning[3,5]

Affiliations:

[1] Department of Ecology and Evolution, University of Chicago, Chicago, Illinois, USA
[2] Department of Science and Technology Studies, York University, Toronto, Canada
[3] Laboratory of Malaria and Vector Research, National Institute of Allergy and Infectious Diseases, National Institutes of Health, Rockville, Maryland, USA
[4] Chan Zuckerberg Biohub, San Francisco, California, USA
[5] International Center of Excellence in Research, National Institute of Allergy and Infectious Diseases, National Institutes of Health, Phnom Penh, Cambodia
[6] Chan Zuckerberg Initiative, San Francisco, California, USA
[7] National Center for Parasitology, Entomology, and Malaria Control, Phnom Penh, Cambodia
[8] Center for Computational Biology, University of California, Berkeley, California, USA
[9] Department of Population Health and Disease Prevention, University of California, Irvine, California, USA
[10] Department of Epidemiology and Biostatistics, University of California, Irvine, California, USA
[11] Department of Biological Sciences, University of Texas, El Paso, Texas, USA
[12] Department of Integrative Biology, University of California, Berkeley, California, USA

*Corresponding author: Cara E. Brook
Email: cbrook@uchicago.edu

Author Contributions: CEB and JEM conceived the study. JEM, JAB, HR, RL, and SC conducted the febrile surveillance study and collected samples for mNGS in 2019-2022. VA, CMT, JLD, JAB, SC, SL, CY, OM, SM, and JEM carried out RT-qPCR to identify dengue-positive samples, as well as library preparation and mNGS. Other ancillary demographic data collection and analyses were performed by RL, KS, CY, FO, and ARP. DP, CL, and JEM set up geospatial system for patients. CEB and JAB generated consensus dengue genomes for upload to NCBI.

CEB carried out all TSIR, FOI, phylogenetic, and simulation analysis, with help from KY, YL, GN, CR, and MB. CR and CEB extended the catalytic model to include waning multitypic immunity. CEB and JEM wrote the first draft of the manuscript. All authors approved and contributed to subsequent drafts of the manuscript and agree with the results presented.

Competing Interest Statement: No competing interests.
Classification: Biological Sciences / Population Biology
Keywords: dengue, genomic epidemiology, force of infection, wavelet decomposition

This PDF file includes:

Main Text
Figures 1 to 5

ABSTRACT

The incidence of dengue virus disease has increased globally across the past half-century, with highest number of cases ever reported in 2019. We analyzed climatological, epidemiological, and phylogenomic data to investigate drivers of two decades of dengue in Cambodia, an understudied endemic setting. Using epidemiological models fit to a 19-year dataset, we first demonstrate that climate-driven transmission alone is insufficient to explain three epidemics across the time series. We then use wavelet decomposition to highlight enhanced annual and multiannual synchronicity in dengue cycles between provinces in epidemic years, suggesting a role for climate in homogenizing dynamics across space and time. Assuming reported cases correspond to symptomatic secondary infections, we next use an age-structured catalytic model to estimate a declining force of infection for dengue through time, which elevates the mean age of reported cases in Cambodia. Reported cases in >70 year-old individuals in the most recent 2019 epidemic are best explained when also allowing for waning multitypic immunity and repeat symptomatic infections in older patients. We support this work with phylogenetic analysis of 192 dengue virus (DENV) genomes that we sequenced between 2019-2022, which document emergence of the DENV-2 Cosmopolitan genotype into Cambodia. This lineage demonstrates phylogenetic homogeneity across wide geographic areas, consistent with invasion behavior and in contrast to high phylogenetic diversity exhibited by endemic DENV-1. Finally, we simulate an age-structured, mechanistic model of dengue dynamics to demonstrate how expansion of an antigenically distinct lineage that evades preexisting multitypic immunity effectively reproduces the older-age infections witnessed in our data.

CLINICAL TRIAL NUMBERS: NCT04034264 and NCT03534245.

SIGNIFICANCE STATEMENT

The year 2019 witnessed the highest number of dengue cases ever reported, including in Cambodia, a Southeast Asian country with endemic transmission. We analyzed 19 years of national dengue surveillance data for Cambodia to demonstrate how increasing temperature and precipitation enhance spatiotemporal synchronicity in epidemic years. We document how two decades of demographic transition has increased the age of reported dengue infection and correspondingly depressed the force of infection through time. We show that introduction of a divergent DENV-2 genotype in Cambodia in 2019 likely drove repeated symptomatic infections in older-age individuals that contributed to a high burden epidemic. As climates warm, we anticipate more synchronized dynamics globally and a shifting burden of symptomatic disease into older cohorts.

MAIN TEXT

INTRODUCTION

Dengue virus (DENV) transmission has increased dramatically over the past two decades, culminating in 2019 with the highest number of global cases ever reported (>5.2 million) to the World Health Organization (WHO) (1). Since nearly three-quarters of DENV infections are estimated to be clinically inapparent (thereby unreported), these counts represent a vast underestimate of the true scale of dengue burden (2). DENV is a flavivirus primarily transmitted by the *Aedes aegypti* mosquito, an ubiquitous arthropod vector in tropical and subtropical regions (2). DENV is comprised of four antigenically distinct serotypes—each of which is further subdivided among four to seven distinct genotypes; infection with one serotype is thought to result in lifelong immunity to that same serotype (homotypic immunity) but only temporary (up to two-year) protection against different serotypes (heterotypic immunity) (3). Heterotypic secondary infections are often more clinically severe due to an interaction with pre-existing flavivirus-specific antibodies known as antibody-dependent enhancement (ADE) (4, 5). Southeast Asia (SEA) reports ~70% of dengue cases globally (1). Historically, dengue has been classified as an urban disease, though recent studies highlighting the importance of microscale transmission in generating DENV diversity in urban Bangkok predict that DENV transmission will intensify across SEA as peri-urban settings become better connected (6–8). Cambodia, at a population size of 16 million, is currently the least urbanized country in SEA (9) but exhibits significant peri-urban sprawl surrounding major metropolitan centers like the capital city, Phnom Penh (6, 7, 9). Urbanization and climatic changes are increasing the population at-risk for dengue in Cambodia and elsewhere (10–12).

Dengue was first detected in Cambodia in 1963 (13), though political instability and civil war in the late 1970s delayed formalization of a passive surveillance policy until 1980 (14). Once adopted, this policy required reporting of clinically diagnosed cases from public health centers and hospitals to the national level. In 2001, the National Dengue Control Program (NDCP) was

135 inaugurated in Cambodia, and in 2002, the NDCP formally implemented the WHO clinical case
136 definitions of dengue and its complications as criteria for the surveillance program (14, 15). The
137 NDCP surveillance system is largely limited to clinicosyndromic diagnoses, meaning that
138 documented cases often correspond to more severe heterotypic secondary DENV infections (16),
139 which are reported collectively without the ability to systematically distinguish serotypes (15).
140 Nonetheless, the NDCP also instituted some active surveillance efforts in Cambodia in 2001,
141 which included limited molecular testing to identify distinct serotypes at sentinel sites in four
142 provinces, which were expanded to 15 provinces by 2021 (14, 15).

143 Over the past two decades, all four dengue serotypes have been detected in Cambodia
144 by molecular surveillance (15), though cases have been largely dominated by one or two
145 serotypes in a given year—with DENV-1 and DENV-3 most common in the early 2000s and
146 DENV-1 and DENV-2 predominant in the last decade (15). Cambodia witnessed three major
147 dengue epidemics across this period–in 2007, 2012, and 2019 (15). The first epidemic, in 2007,
148 occurred coincidentally with a genotype replacement event in DENV-1 (17, 18), though cases
149 were dominated by DENV-3, marking the last year of this serotype's dominance in the region (14,
150 18). The second epidemic, in 2012, has been largely attributed to DENV-1 (15, 19–21), and the
151 third, in 2019, appears to have been driven by co-circulation of both DENV-1 and DENV-2 (15).
152 Consistent with the global trends (1), Cambodia suffered its worst dengue epidemic on record in
153 2019, with approximately 40,000 total cases reported across all 25 provinces—a likely drastic
154 underestimation of the true disease burden (22). The past twenty years of surveillance in
155 Cambodia have witnessed, on average, steadily increasing dengue incidence, coupled with a
156 steady increase in the mean age of reported dengue infection (15). The increased age of reported
157 infection has been anecdotally attributed to an aging population following demographic transition,
158 as similar phenomena have been documented previously in neighboring Thailand (23, 24) and in
159 Nicaragua (25).

160 Explosive periodic outbreaks are a hallmark of dengue virus disease, though the multiple
161 drivers of these phenomena have long been debated (24, 26–29). Seasonal climate cycles are a

162 strong predictor of annual cycling for many arboviruses, including dengue (10, 11), and climate
163 has been implicated as a possible driver of multiannual dengue periodicity, as well. In Thailand,
164 multiannual dengue cycles demonstrate coherence with El Niño phenomena (29), and epidemic
165 years exhibit more synchronized dynamics across latitudes (29), as well as higher correlation with
166 local temperature than do inter-epidemic periods (28). The interaction of demography and
167 heterotypic immunity is also thought to play a role in driving multiannual dengue cycles (24, 26,
168 30), which, in Thailand, show elongated periodicity as a result of declining birth rates and slower
169 build-up of the susceptible population over the past half-century (24). Virology also contributes to
170 dengue epidemics, which have, historically, been linked to turnover in the dominant regional
171 serotype (31–33) or to replacement of a dominant viral genotype within a single serotype (18, 34).
172 Genotype-specific antigenic diversity is increasingly recognized within traditional serotype
173 classifications for dengue (35), and recent work links the magnitude of periodic dengue epidemics
174 to this antigenic evolution (34, 35). Large epidemics tend to result from the takeover of DENV
175 lineages most antigenically distinct from previously circulating strains of the same serotype or
176 most antigenically similar to lineages of a different serotype (34).

177 Here, we explore the dynamics of dengue virus transmission across the past two
178 decades in peri-urban Cambodia, investigating the potential mechanisms that underly periodic
179 epidemics, particularly the epidemic of 2019. We queried a 19-year dataset (2002-2020) of
180 serotype-agnostic dengue case counts from the NDCP, aggregated at the province level, to, first,
181 interrogate the role that climate played in driving epidemics in 2007, 2012, and 2019, and second,
182 more generally, explore the impact of climate on annual and multiannual cycling across the time
183 series. We, third, fit catalytic models to the age-structured incidence of reported dengue disease
184 to estimate the annual force of infection (FOI), at the province level, across this time series (24,
185 36, 37), then considered the national data in the context of our own active febrile surveillance
186 study carried out in peri-urban Kampong Speu and surrounding provinces from 2019-2022 (38).
187 Whole genome sequencing of DENV from serum samples collected in our active surveillance
188 program, combined with additional sequences from NDCP surveillance, identified the first record

189 of the DENV-2 Cosmopolitan lineage ever documented in Cambodia (39). Phylodynamic analysis
190 of the spread of the DENV-2 Cosmopolitan lineage in this region suggests that this genotype
191 caused pathogenic infections in older age individuals, contributing to the largest documented
192 dengue outbreak on record for Cambodia in 2019. Finally, we constructed an age-structured
193 discrete-time, dynamical model to simulate the interplay of climate, demography, immunology,
194 and virology which combine to structure two decades of dengue dynamics in Cambodia.
195

196 **RESULTS**

197 **Though warming temperatures correlate with increasing dengue incidence in Cambodia,**
198 **epidemic years are not consistent climate anomalies.**

199 Because of the widely acknowledged role of climate as a driver of arboviral disease
200 globally (10, 11), coupled with recent work from Thailand that highlights coherence between El
201 Niño climate anomalies and dengue epidemics (29), we first explored the influence of changing
202 temperature and precipitation on dengue caseload in Cambodia. To this end, we aggregated
203 high-resolution temperature and precipitation data at the Cambodian province level, across two-
204 week intervals from 2002-2019 and sought to address the extent to which epidemic years
205 represented climatic anomalies over this time period; we defined 'anomalies' as any years in
206 which temperature or precipitation records demonstrated significant deviations from average
207 trends through time, as calculated using generalized additive models (GAMs) (40). Across the
208 time series, temperature peaked in the first half of each year, between April and July, preceding
209 the peak in dengue caseload (Fig. S1). Precipitation peaked in the latter half of each year,
210 between August and October (Fig. S2), preceding the onset of the following year's dengue
211 season. GAMs (40) demonstrated that, after controlling for intra-annual variation, temperature
212 has increased significantly across the past two decades in all provinces; no significant interannual
213 changes were detected for precipitation (Fig. S3-S4; Table S1). Additional GAMs and climate
214 data normalized into z-scores indicated that the epidemic years of 2012 and 2019 were
215 anomalously warm, while 2007 was anomalously cool, consistent with the observed interannual

216 increase in temperature (Fig. S5). Years 2015-2016, which spanned a major El Nino event in
217 SEA (but did not correspond to a dengue epidemic in Cambodia) (41), were also significantly
218 warmer than average. By contrast, precipitation showed no anomalies in the year preceding each
219 of the three major dengue epidemics (Fig. S6). We concluded that, while both temperature and
220 dengue incidence increased across our time series, epidemic years could not be consistently
221 distinguished by any consistently aberrant climatic profile.
222
223 **Climate-informed transmission rates failed to recover epidemic dynamics in a TSIR model.**
224 To formally interrogate the role of climate as a driver of dengue epidemics in Cambodia,
225 we developed a simple, climate-informed time series Susceptible-Infected-Recovered (TSIR)
226 model (42–44), which we fit to dengue case counts, aggregated over two week intervals at the
227 province level, for the three inter-epidemic periods (2002-2006, 2008-2011, and 2013-2018).
228 Typically used to describe the transmission dynamics of perfectly immunizing childhood
229 infections, such as measles (43, 44), TSIR has been applied to dengue dynamics previously and
230 offers an effective means by which to isolate the impact of climate on transmission, despite
231 oversimplifying the multiple serotype dynamics of dengue virus disease (45–49).
232 We used biweekly transmission rates recovered from TSIR fits to the inter-epidemic
233 periods, as well as climate-informed transmission rates for epidemic years projected from
234 province-specific lagged temperature and precipitation data, to predict epidemic-year cases (Fig.
235 1; *Methods; SI Appendix*). We found that TSIR successfully recaptured the timing of annual
236 dengue epidemics across the 22 provinces considered, with the recovered transmission rate
237 peaking between May and August, slightly preceding reported cases. The magnitude and timing
238 of transmission varied by province and between the three inter-epidemic periods, showing no
239 consistent pattern of directional change in magnitude with time (Table S2). TSIR-estimated
240 transmission was significantly positively associated with higher temperature and precipitation
241 (lagged such that climate variables preceded transmission by a median 3.5 months for
242 temperature and 1 month for precipitation) in the corresponding province across all inter-epidemic

periods (Table S3-S4). More rapid transmission gains were observed for corresponding increases in temperature vs. precipitation (Fig. S7-S9; Table S4). Nonetheless, climate-informed transmission rates for epidemic years were not substantially different from rates fitted to inter-epidemic periods, reflecting the absence of major climate anomalies across the time series (Fig. S10).

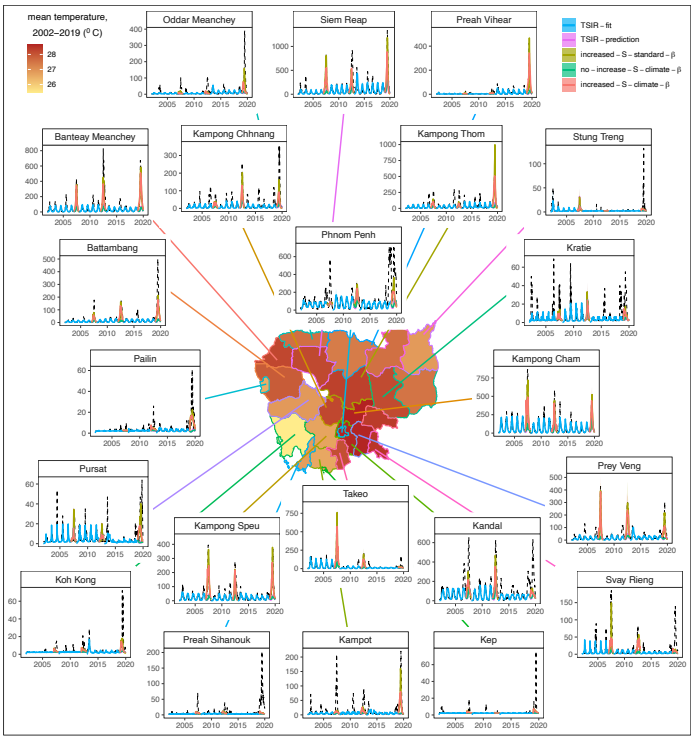

Figure 1. Climate-informed TSIR insights into epidemic dynamics of DENV in Cambodia. Inset panels show province level clinicosyndromic reported DENV cases (*dashed black lines*) with fitted TSIR output to the three inter-epidemic periods (2002-2006, 2008-2011, 2013-2018; *blue lines*) and TSIR projections for epidemic years (2007, 2012, 2019) under trained biweekly transmission rate (β) estimates (*pink lines*), incorporating a factorial increase in the susceptible population (*gold lines*), using a climate-projected β estimated from lagged temperature and precipitation data by province (*green lines*), or using both climate-projected β and a factorial increase in the susceptible population (*red lines*) (*SI Appendix,* Table S2, S5). The center map shows province level administrative boundaries for Cambodia, shaded by the mean biweekly temperature in 2020.

As expected, TSIR underpredicted the magnitude of epidemic year caseloads for all provinces; climate-informed transmission improved TSIR projections but still failed to recover epidemic peaks (Fig. 1). Experimentally, we amplified the susceptible population input at the beginning of each epidemic year in our model, which facilitated recovery of DENV caseloads

264 (*Methods*) (49). In the absence of climate input into the transmission rate, the proportional
265 increase in susceptible population at the beginning of each epidemic year needed to recover the
266 epidemic peak was a median 1.8x for 2007, 2.10x for 2012, and 2.17x for 2019 (Table S5). The
267 proportional increase in the susceptible population needed to recover the epidemic peak was not
268 significantly lower when epidemic year cases were projected using climate-informed transmission
269 rates for 2007 and 2012 (paired student's t-test: [2007] $t=0.33$, $p>0.1$; [2012] $t=-0.52$;$p>0.1$) and
270 only marginally lower for 2019 ($t=1.31$, $p=0.1$), suggesting (at most) a minimal role for
271 temperature and precipitation in driving epidemic dynamics (Table S5). For many provinces, the
272 combination of climate-informed transmission rate with susceptible augmentation still fell short of
273 effectively capturing epidemic caseloads, highlighting the need for alternative explanations for
274 these high transmission years.
275
276 **Wavelet analysis showed enhanced synchrony in dengue dynamics across provinces and**
277 **climate time series in epidemic years.**
278 Though TSIR modeling failed to recover a clear role for climate in driving major dengue
279 epidemics in Cambodia, the analysis did highlight a critical influence of climate on the intraannual
280 timing of cases and the interannual periodicity of dengue dynamics. Prior work in Thailand has
281 demonstrated enhanced synchronicity between dengue incidence and climate, and between
282 geographically distant localities, during major epidemics (28, 29), as well as a link between
283 multiannual climate cycles and higher burden epidemics (29). We hypothesized that these
284 multiannual climate cycles not considered in TSIR might also be important in the Cambodia
285 system. To this end, we undertook wavelet decomposition of the biweekly dengue time series and
286 the corresponding climate data, both at the province level, to extract and disaggregate annual
287 and multiannual trends. We found elevated amplitude and statistically significant peaks in
288 average wavelet power of both annual (Fig. 2A, S11A) and multiannual (Fig. 2B, S11B) cycles in
289 dengue incidence during the three epidemic years (50). Elevated amplitudes for multiannual
290 cycles were also observed during the 2015-2016 El Niño event in more northerly provinces (Fig.

2B), including those abutting Thailand, where associations between dengue and El Niño have been previously established (29). We additionally observed significantly elevated synchronicity between provinces in the timing and amplitude of yearly dengue incidence across epidemic years, as measured both by pairwise Pearson's correlation coefficient (Fig. 2C) and cross-wavelet power (Fig. S11). Synchronicity in the annual incidence data was negatively associated with geographic distance between provinces, though patterns were less clear than have been described elsewhere (29) (Fig. S12). High synchronicity between annual case data for paired provinces was significantly positively associated with high temperature, precipitation, and population size of a focal province (Fig. S12; Table S6).

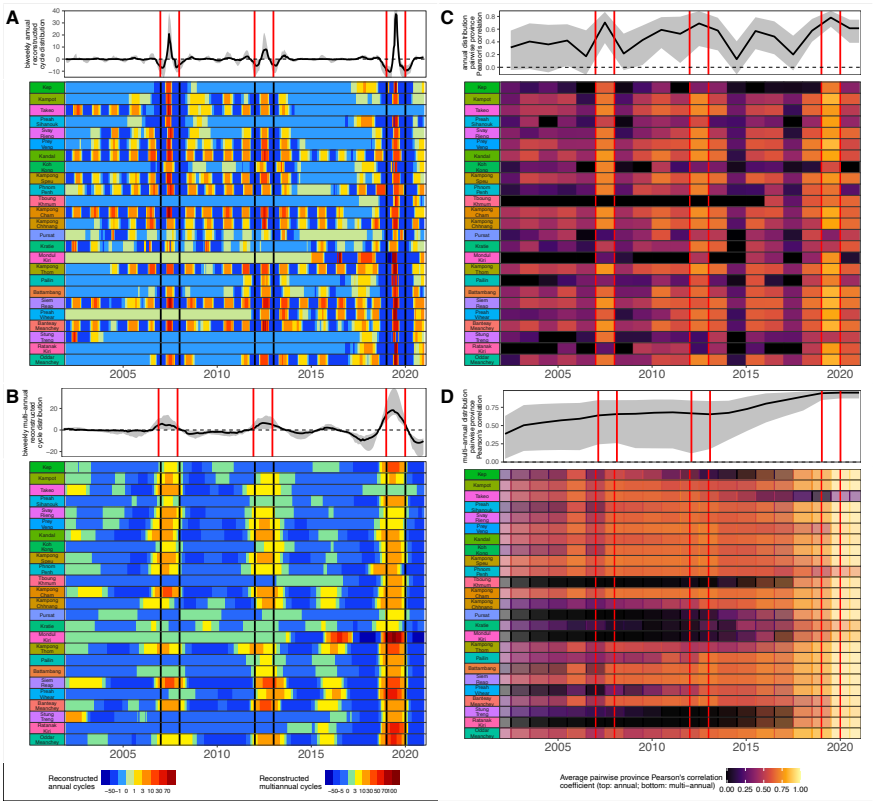

Figure 2. Wavelet reconstructions show heightened synchrony in epidemic years. Reconstructed **A** annual and **B** multiannual dengue cycles by province, by year from NDCP incidence per 100,000 population. **C** Mean pairwise Pearson's correlation coefficient (ρ) for annual dengue incidence between focal province and all other provinces through time. **D** Mean ρ comparing province-to-province reconstructed multiannual dengue cycles across a 5-year sliding window, with overlapping window frames plotted (partially translucent) atop one another. In all panels, epidemic years are highlighted by vertical red or black bars. Top panels indicate the distribution of corresponding values (median = solid line; max-to-min range = gray shading) observed across all provinces within each timestep. X-axis labels are marked on January 1 of the corresponding year.

For multiannual cycles, we observed a trend of steadily increasing synchronicity (Fig. 2D) and cross-wavelet power (Fig. S11D) between provinces through time, though no peaks occurred in epidemic years. Cross-wavelet power between raw dengue incidence and the corresponding, province-level mean temperature and total precipitation (grouped biweekly) also peaked in epidemic years (Fig. S13 AB). At the multiannual scale, cross-wavelet power between province-level reconstructed dengue cycles and temperature and precipitation largely increased across the time series (Fig. S13CD), though values were highest slightly preceding the 2019 epidemic and overlapping the 2015-2016 El Niño event (41). The same pattern was observed when comparing monthly reconstructed multiannual dengue cycles and the Oceanic Niño Incidence (ONI) (Fig. S13E). For temperature, precipitation, and ONI, cross-wavelet power with multiannual dengue cycles peaked earlier in the time series in more southern provinces and moved gradually northward (Fig. S13C-E). All told, wavelet analyses suggested a role for climate in synchronizing annual dengue epidemics across provinces, but only minimal support for a hypothesis of multiannual climate cycles driving periodic epidemics across our time series. In contrast to reports from two decades prior in Thailand (24), the periodicity of multiannual dengue cycles across provinces did not increase in duration throughout our time series, despite decreasing birth rates (Fig. S14). This perhaps reflects the relative slowdown in both birth and death rate declines in Cambodia over the past two decades, when compared with the dramatic declines witnessed twenty years prior (Fig. S14).

Mean age of reported dengue infection increased across the study period, corresponding to a declining force of infection.

The muted effects of climate on our epidemic time series led us to next investigate demographic and immunological drivers of dengue dynamics in Cambodia. Previous work has documented a trend of increasing mean age of reported dengue infection across the past two decades in Cambodia at the national level (15); we confirmed this to be consistent at the province level (Fig. 3A,B; Fig. S15; Table S7). Nationally, the mean age of reported dengue infection

increased from 6.79 years (95% CI: 5.85-7.72) in 2002 to 10.34 years (95% CI: 9.41-11.27) in 2020 ($p<0.001$). Increases in age of reported cases were even more dramatic in more remote provinces: in the distant northeastern province of Mondul Kiri, for example, the mean reported age of infection increased from 3.72 years (95% CI: 1.97-5.47) in 2002 to 21.18 years (95% CI: 20.84-21.53) in 2020 (Fig. 3A; Fig. S15; Table S7).

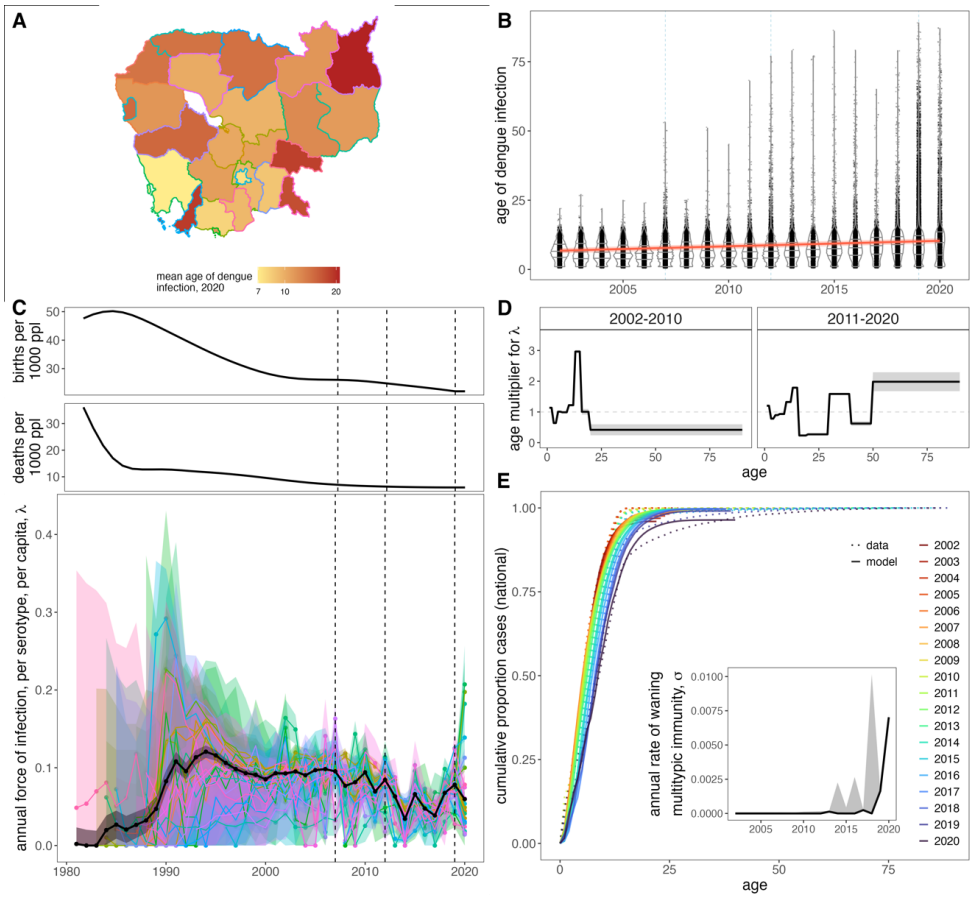

Figure 3. Demographic transition underpins declining force of infection and increasing age of reported dengue incidence in Cambodia. A Mean age of reported dengue infection, by province in the last year of the NDCP time series (2020). **B** Age distribution of reported dengue cases by year, with violin plots highlighting changes in the interquartile range of cases. The interannual trend in the mean age of dengue infection is plotted as a solid red line, with 95% confidence intervals by standard error shown as a narrow, translucent band behind it (Table S7). Epidemic years (2007, 2012, 2019) are highlighted by a light blue, dashed line in the background. **C** National (black) and province level (colored) estimates for the annual, per serotype, per capita force of infection from 1981 to 2020. 95% confidence intervals from the hessian matrix are shown as translucent shading. FOI estimates are compared against national birth and death rates for Cambodia across the time series, with epidemic years highlighted by vertical dashed lines. **D** Age modifiers to the FOI fit as shared across all provinces for 2002-2010 and 2011-2020 subsets of the data, with 95% confidence intervals from the hessian matrix are shown as translucent shading. **E** Cumulative increase in the proportion of cases reported by age at the national level, colored by year. Data are shown as dotted lines and model output as solid lines. Model includes national FOI estimates from **C**, age modification terms from **D**, and time-varying waning multitypic immunity as shown in the inset.

361 To interrogate the mechanistic drivers of this pattern, we estimated the annual force of
362 infection (FOI, or λ), the rate at which susceptibles become infected, by fitting a catalytic model
363 with multiple serotype exposures to the province level data for every year in the dataset (2002-
364 2020) and the 22 years preceding the onset of the time series, dating back to the birth year of the
365 oldest individual in the first year of the data (Fig. 3C) (24, 36, 37). As in previous models for
366 dengue (24, 36), we assumed that reported cases represented secondary, symptomatic
367 infections most likely to report to public hospitals and clinics. Resulting patterns in FOI by
368 province largely mirrored those recovered nationally (Fig. S16), demonstrating a consistently high
369 FOI in the early 1990s, corresponding to the years in which individuals born in Cambodia's 1980s
370 birth pulse (which followed severe population reductions from civil war in the 1970s) would likely
371 experience secondary infections. The FOI subsequently demonstrated a gradual decline across
372 the time series, interspersed with local peaks in epidemic years and in 2010 and 2015.
373
374 **Age-structured FOI modifications and waning multitypic immunity in 2019-2020 improved**
375 **the catalytic model's ability to recapture observed data.**
376 We next fit 19 multiplicative age modification parameters, shared across all provinces, to
377 allow for modulation of annual FOI across different age categories; eight age class were
378 considered for the first half of the time series and eleven for the second, corresponding to the
379 expanded age range of reported cases (Fig. 3D). Incorporation of age modifiers improved model
380 fits to the data across all provinces (Table S8). Consistent with recent work in Thailand (23), we
381 identified a high hazard of infection in adolescents (13-15 year-olds) across the time series. In the
382 second decade, we additionally noted an elevated age-specific hazard of infection in 30-39 year-
383 olds and >50 year-olds, corresponding to case reports in older cohorts.
384 Because the age range of these older cases greatly exceeded average age increases
385 predicted by declining FOI, we reconsidered our original assumption by which reported cases
386 corresponded to clinically apparent secondary infections only. Visualization of the age distribution
387 of reported cases by year at both the national (Fig. 3B) and province levels (Fig. S15) indicated

388 that, in addition to increases in the mean reported age of dengue infection, the past two decades
389 of dengue incidence in Cambodia have also witnessed expansion in the age *range* of reported
390 cases—such that approximately 1% of reported cases (712/68597) in 2019 occurred in
391 individuals over the age of 45, with 61 infections reported in individuals >70 years in age. We also
392 observed an isolated spike in the age distribution of reported cases in some provinces in the
393 epidemic years of 2007 and 2012 (Fig. S15). To recapture these symptomatic infections in older
394 age-individuals, we modified the multitypic catalytic modeling framework presented in previous
395 work (24, 25, 36) to permit individuals to wane from a state of multitypic immunity back to that of
396 monotypic immunity subject to renewed hazard of symptomatic re-infection (*SI Appendix*). Using
397 this new modeling framework, we estimated a shared parameter across all provinces, which
398 corresponded to the rate of waning multitypic immunity (σ). When we allowed σ to vary by year,
399 we estimated a significant signature of waning multitypic immunity in the 2019 and 2020 data only
400 (Fig. 3E, *inset*). Incorporating time-varying σ improved model fit when added both to the FOI-only
401 model and the FOI model modified by age class (Table S8). Our best fit FOI model including both
402 age modifications and time-varying multitypic waning immunity effectively recaptured the
403 observed cumulative proportion of cases per age class per year at national (Fig. 3E) and province
404 (Fig. S17) levels. In general, cases accumulated more slowly across age classes with advancing
405 years, tracking declining FOI.
406
407 **DENV genotyping from 2019-2022 suggests a likely DENV-2 clade replacement event in**
408 **Cambodia.**
409 The results of our FOI analysis led us to question whether regional turnover in the
410 dominant DENV virus lineage could underpin the 2019 signature of immunological nativity
411 identified in our data. Prior work emphasizes the key role that antigenic novelty, influenced by
412 both serotype and genotype, plays in determining fitness advantages for co-circulating DENV
413 variants (34, 35). To address this question in our system, we leveraged serum samples amassed
414 during an active febrile surveillance study that we carried out in Kampong Speu province,

adjacent to the Cambodian capital city of Phnom Penh, between July 2018 and December 2022 (38, 39). In this study, serum collected from patients reporting to the provincial referral hospital within 24 hours of fever was subject to RNA extraction and metagenomic Next Generation Sequencing (mNGS) to identify the etiology of infection (38, 39). We successfully identified serotype and corresponding genotype from mNGS data for 239 DENV-positive Kampong Speu cases. We supplemented these with samples collected from 11 cases identified in our more limited active surveillance in five neighboring provinces in 2021-2022 and 20 cases identified in routine NDCP surveillance across six provinces, also in 2021-2022 (Fig. 4A; Table S9). From this data subset of positive DENV samples, we sequenced and submitted 192 whole DENV genomes to NCBI (63 DENV-1, 120 DENV-2, and 9 DENV-4; Table S9), representing one-third of full genome DENV-1 sequences and two-thirds of full genome DENV-2 sequences currently available for Cambodia.

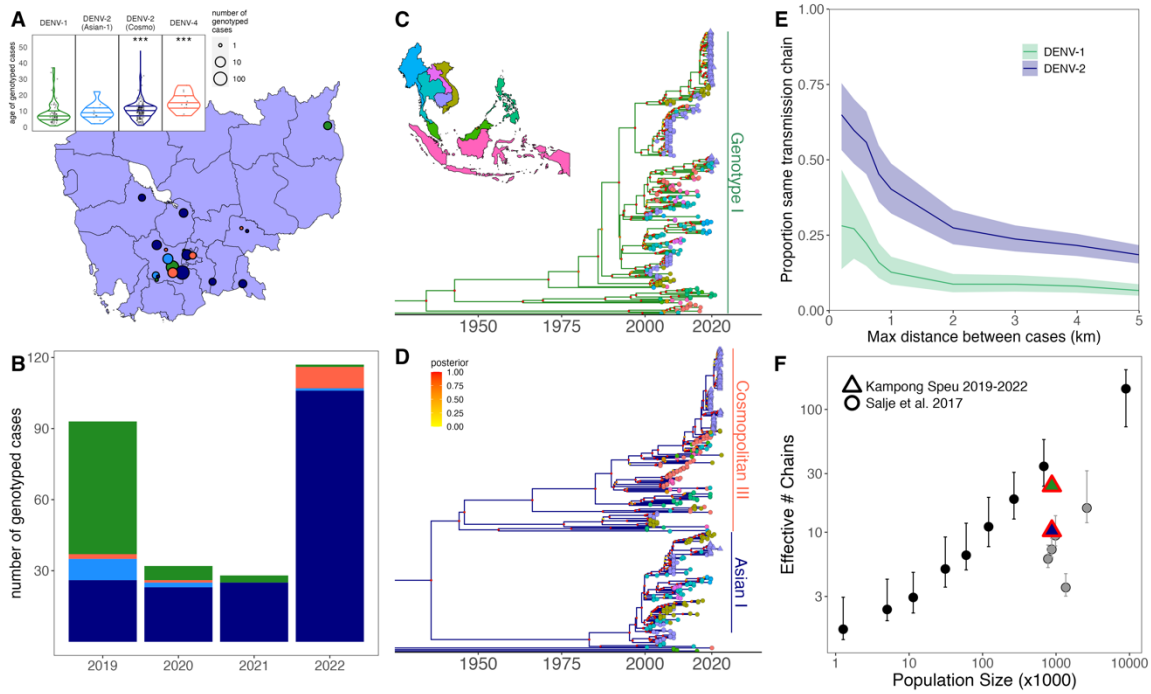

Figure 4. Bayesian time trees highlight geospatial structuring in evolutionary relationships for Cambodian dengue. A Map of Cambodia with locations of DENV serum samples genotyped from 2019-2022 in part with this study. Cases are grouped together within 10km radii. The centroid of each case cluster is plotted, with circle size corresponding to sample number and shading corresponding to serotype and genotype (DENV-1=green; DENV-2 Asian 1= light blue; DENV-2 Cosmopolitan = navy; DENV-4=orange). The age distribution of cases by serotype and genotype is shown in the upper left; DENV-2 Cosmopolitan and DENV-4 infections occurred in significantly older age individuals than reference DENV-1 infections

(linear regression; p<0.001; Table S10). **B.** Number of genotyped DENV cases by year from febrile surveillance in this study, colored by serotype and genotype as showing in panel A. **C** Map of Southeast Asia with countries colored corresponding to sequences, as shown in tip points on phylogenetic timetrees constructed using BEAST 2 for DENV-1 and **D** DENV-2. X-axis highlights divergence times between corresponding sequences. Reference sequences from GenBank are represented as circle tips and sequences contributed by active febrile surveillance in this study as triangles. Cambodia and corresponding sequences are shaded purple. Clade bars indicate the genotype of corresponding sequences within each serotype: genotype-1 for DENV-1 and Asian-1 and Cosmopolitan III for DENV-2. See Fig. S19 for a detailed inset of geographic localities for 2019-2022 Cambodia sequences. **E** Proportion of geolocated sequence pairs from panel A for DENV-1 (*green*) and DENV-2 (*blue*) genomes derived from the same transmission chain across progressively longer Euclidean distances. **F** Number of effective transmission chains for circulating DENV estimated across populations of varying densities. Black (urban) and gray (rural) circles with corresponding 95% confidence intervals depict estimates for Thailand from Salje et al. 2017 (8), while triangles depict estimates from our Kampong Speu active febrile surveillance study for DENV-1 (*green*) and DENV-2 (*blue*).

Maximum likelihood phylogenetic analysis of the resulting genomes demonstrated that most DENV-2 sequences recovered from our 2019-2022 study belonged to the DENV-2 Cosmopolitan III lineage, the first record of this genotype in Cambodia, though its emergence has been reported recently in several neighboring SEA countries (Fig. S18) (51–54). All DENV-1 sequences clustered in the Genotype 1 lineage, consistent with previous genotype records in Cambodia (Fig. S18). Genotyped cases from 2019 were largely split between DENV-1 (N=56/93, 60.2%) and DENV-2 (N=35/93, 37.6%) serotypes, while those from 2020-2022 were dominated by DENV-2 (2020: N=25/32, 78.1%; 2021: 25/28, 89.3%; 2022: 107/117, 91.4%) (Fig. 4B). A small number of DENV-4 cases were also sequenced across the time series (Fig. 4B). The Cosmopolitan III lineage of DENV-2 became increasingly prevalent across the time series, as compared with the Asian 1 genotype previously recorded in Cambodia (Fig. 4B). The Cosmopolitan lineage increased in prevalence from 74.3% (26/35) of DENV-2 cases in our study in 2019 to 99.1% (106/107) of cases in 2022 (Fig. 4B). We additionally observed that the mean age of infection was significantly higher for DENV-2 Cosmopolitan cases genotyped in our study (while the mean age of DENV-2 Asian 1 infection showed no difference), as compared with reference DENV-1 case (Fig. 4A; Table S10, p<0.001). Mean age of infection was also significantly elevated for DENV-4, likely because it circulated at much lower prevalence.

We constructed serotype-specific Bayesian timetrees (55, 56) from full genome DENV sequences to assess the divergence time of 2019-2022 lineages from sequences previously reported from Cambodia and neighboring SEA countries between 2002-2022 (Fig. 4C-D; Table

472 S9). The majority of DENV-1 lineages recovered from our study in 2019-2022 clustered closely
473 with other DENV-1 sequences reported to NCBI from Cambodia across the past decade (Fig.
474 4C). By contrast, DENV-2 sequences in the Cosmopolitan III lineage demonstrated high
475 divergence from the most recently reported Asian-1 sequences for Cambodia, with a time to most
476 recent common ancestor (tMRCA) of approximately 77.1 years (Fig. 4D; MRC: 1945, 95% HPD:
477 1942-1949). Locally, within our regional data subset, sequences collected from cases coincident
478 in geographic space and time were highly phylogenetically related (Fig. S19), supporting previous
479 studies emphasizing the importance of microscale transmission for DENV (8). Nonetheless, we
480 observed reduced phylogenetic diversity overall and a higher degree of phylogenetic relatedness
481 across wider geographic distances for DENV-2 vs. DENV-1 sequences, consistent with a
482 hypothesis of recent genotype invasion (Fig. 4E). Indeed, some 60% of paired DENV-2
483 sequences separated by up to 400m of geographic distance were estimated to share a MRCA
484 within six months of the onset of the earlier case (corresponding to a shared 'transmission chain'),
485 as compared with only 22% of DENV-1 sequences. At a distance of up to 1 km separation, some
486 40% of DENV-2 pairs still belonged to the same transmission chain, in contrast to only 13% of
487 DENV-1 sequences. Specifically for the Kampong Speu data, we additionally estimated the
488 number of distinct DENV-2 vs. DENV-1 effective transmission chains in circulation in the region
489 (Fig. 4F). When compared with prior work from neighboring Thailand, the number of effective
490 transmission chains per population size for DENV-1 in Kampong Speu closely matched that
491 predicted by population size in the endemic transmission setting of urban Bangkok (8). By
492 contrast, the lower number of transmission chains per population size estimated for DENV-2 was
493 closer to that previously observed in rural regions in Thailand with less continuous endemic
494 transmission (Fig. 4F).

495 All told, our phylogenetic analyses describe the emergence of a previously unrecorded
496 genotype of highly divergent DENV-2 in at least ten different Cambodian provinces. This
497 genotype greatly increased in prevalence following its first record in Cambodia in 2019 and
498 caused infections in older-age individuals. The limited phylogenetic diversity observed from

499 DENV-2 sequences suggest that the Cosmopolitan lineage arrived relatively recently to the
500 region. Its high genetic divergence from previously reported genotypes in Cambodia may be
501 associated with antigenic novelty that played a role in the 2019 epidemic.
502
503 **Mechanistic simulations of clade replacement with antigenic escape in an age-structured**
504 **model recapture patterns witnessed in the data.**
505 Combined, our FOI analysis and genotyping suggest that the DENV-2 Cosmopolitan
506 lineage caused a genotype replacement event in Cambodia, which likely played a part in the
507 2019 epidemic in the region. The higher burden of cases in older age individuals more likely to
508 have some form of pre-existing dengue immunity additionally suggested that the Cosmopolitan
509 genotype may be sufficiently antigenically divergent to overcome this immunity, resulting in
510 symptomatic infection. To formally evaluate this hypothesis, we constructed a mechanistic, age-
511 structured discrete time deterministic epidemic model in biweekly timesteps (*SI Appendix*) (57–
512 59), with which we simulated diverse mechanisms hypothesized to underpin observed patterns in
513 our data. We sought to explain both the general pattern of increasing average age of reported
514 infection through time, as well as the high caseload and wide distribution in age range of cases
515 associated with the 2019 epidemic (and, to a lesser extent, prior epidemic years). Previous work
516 in Thailand shows similar patterns of drastically older age infections in more recent years, which
517 the authors explain via a mechanism of increased detectability of tertiary or quaternary infections
518 through time (23). In practice, this mechanism is similar to our extension of Ferguson et al.
519 (1999)'s catalytic model for dengue, which incorporates waning multitypic immunity, as both
520 approaches allow for case detection in individuals experiencing more than two dengue infections
521 across their lifetime. We used our simulation model to evaluate whether these two mechanisms
522 were functionally distinguishable and, if so, which best replicated Cambodian data.
523 For simplicity, we restricted ourselves to a three-serotype system and initiated
524 simulations incorporating seasonal variation in transmission as estimated by TSIR (Fig. 1) and
525 annual variation in FOI corresponding to national estimates (Fig. 3). As with our FOI analysis, we

modeled secondary infections as reported cases for (H0) normal demographic simulations. We then compared these results against simulations of (H1) hypotheses that allowed for continuously increasing detectability of tertiary cases through time or (H2) hypotheses of genotype replacement paired with waning multitypic immunity and detectable reinfection within a serotype (Fig. 5). We also compared (H3) hypotheses of genotype invasion with no lineage-specific changes in immunology or (H4) hypotheses of genotype invasion with continuous increasing tertiary case detection, again not specific to the invading lineage (Fig. S21). We focused our analyses on drivers of the 2019 epidemic but also conducted a subset of simulations to highlight insights gleaned from the 2007 epidemic in Cambodia (Fig. 5, *bottom*).

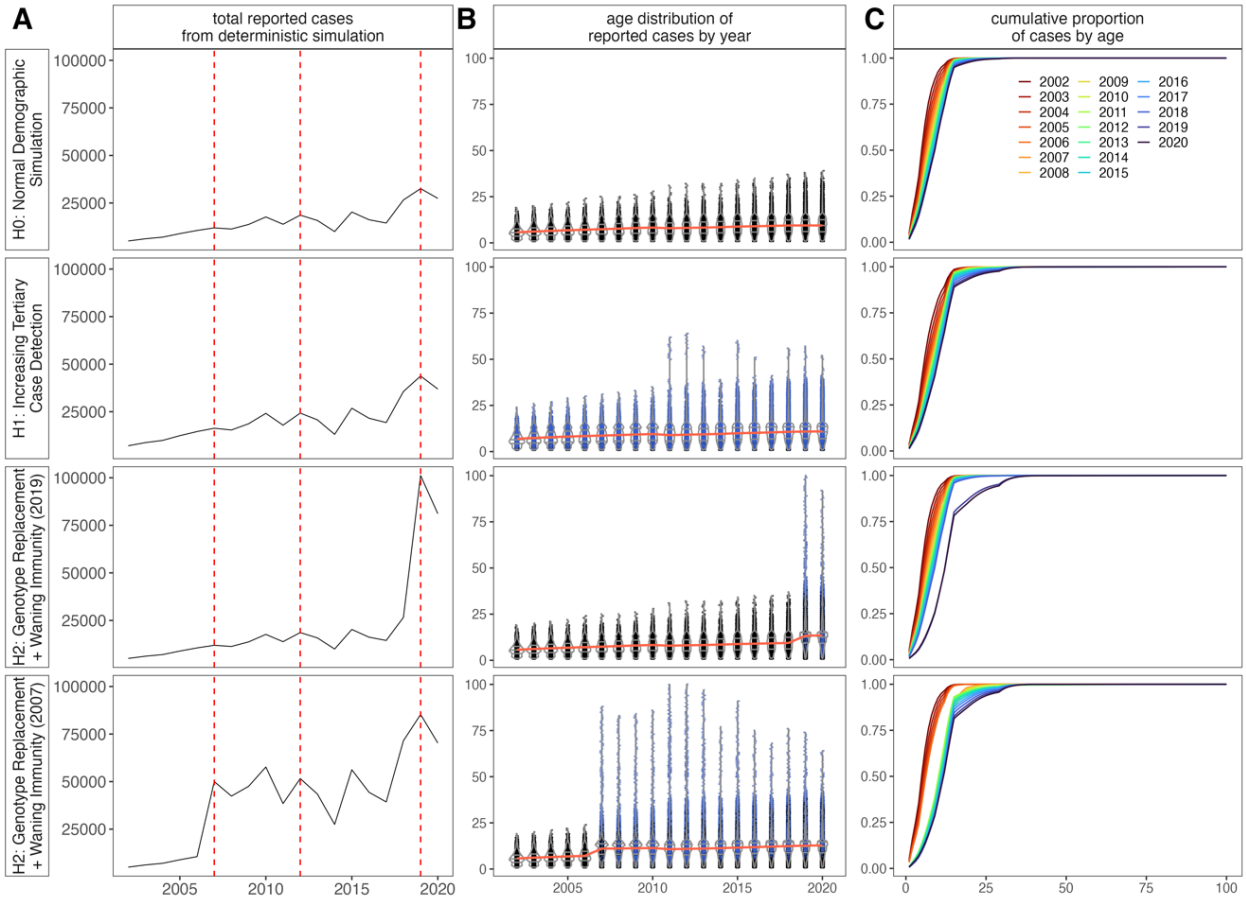

Figure 5. Simulations of genotype clade replacement recapitulate observed expansion in the age structure of reported dengue cases from Cambodian data. A Total reported cases (solid line = mean FOI; translucent shading = 95% confidence interval for FOI), **B** age distribution of reported cases by year (black = secondary; blue = repeat secondary or tertiary), and **C** cumulative proportion of reported cases by age, from deterministic model simulations indicated to the left of panel A.

542 All simulations successfully recovered the pattern of increasing mean age of reported
543 infection, as witnessed in the data. This increase was steeper under (H1) assumptions of
544 increasing detectability for tertiary infections (Fig. 5). Because we parameterized FOI from the
545 national time series for Cambodia, for which the 2019 FOI was locally elevated (Fig. 3), all
546 simulations also effectively reproduced a higher burden of cases in 2019. Critically, we found that
547 sudden, sharp expansions in the age distribution of reported cases, as witnessed broadly across
548 provinces in epidemic years for Cambodia (Fig. S15), were only possible when modeling some
549 form of antigenic novelty for the invading lineage (H2; Fig. 5). Simulations of this novel antigenic
550 invasion in 2007 (Fig. 5 H2, *bottom*) also demonstrated how the expanded age distribution should
551 subsequently narrow in the years following clade replacement with immune evasion, again
552 consistent with Cambodian data (Fig. S15). By contrast, (H1) hypotheses of constant increasing
553 tertiary case detection through time will only continue to expand this distribution over longer time
554 horizons. Importantly, modeling of genotype turnover had no demonstrable impact on the age
555 distribution of cases in the absence of *specific* enhanced detectability for the invading clade, even
556 when allowing for generally heightened tertiary case detection through time (Fig. S21). Thus, we
557 conclude that only introduction of antigenically divergent genotypes (or, of course, serotypes) can
558 be expected to generate this dramatic short-term expansion in the age distribution of cases.
559 Notably, our results were agnostic to classification of repeat infections with an invading lineage as
560 tertiary detections (e.g. detection of DENV-2 infection following prior exposure to DENV-1 and
561 DENV-4) vs. repeat detections within a serotype (e.g. detection of DENV-2 following prior
562 exposure to a previous lineage of DENV-2). The epidemic consequences of this invasion were
563 comparable, so long as enhanced detectability (e.g. antigenic escape) was specific to invading
564 lineage.
565

566 **DISCUSSION**

567 Drawing from two decades of national surveillance data and a more recent genomic
568 cohort study, we queried the mechanisms that underly dengue virus transmission and drive

569 periodic dengue epidemics in Cambodia. All told, our study highlights the complex interplay of
570 climate, demography, immunology, and virology that dictates the dynamics of dengue virus
571 disease in endemic settings.

572 Our investigations of climate effects on dengue transmission in Cambodia mirror those
573 previously reported in Thailand (28, 29), Sri Lanka (49), and China (45), emphasizing the role of
574 temperature, and—to a lesser extent—precipitation, in synchronizing annual dynamics in
575 epidemic years. Consistent with prior work that highlights a role for El Niño in driving multiannual
576 dengue cycles in other systems (29), we observed synchrony between reconstructed multiannual
577 dengue cycles in Cambodia and the ONI; however, this synchrony appeared to peak during the
578 robust 2015-2016 El Niño, which did not correspond to one of the three major dengue epidemic
579 years in our dataset—though some signature of elevated amplitude for multiannual dengue
580 cycles in northern Cambodia (adjacent to the Thai border) suggest a local epidemic may have
581 occurred during this time. The muted impact of climate on dengue dynamics in Cambodia could
582 reflect overall higher caseloads in association with elevated temperatures in more recent years
583 (28), making any further transmission gains comparatively less dramatic. In addition, climate
584 impacts on DENV transmission may be generally less discernable in Cambodia, which has
585 reduced latitudinal variation (and corresponding climate differences) than other SEA countries,
586 such as Thailand. Nonetheless, our analysis suggests that warmer temperatures play a role in
587 driving epidemic dynamics for Cambodian dengue and likely contributed to high caseloads in
588 2019. As temperatures increase globally, dengue transmission is likely to accelerate, and
589 variation in both timing of annual dengue transmission and multiannual peaks in caseload may
590 become more homogenous.

591 In addition to climate, our data and corresponding analysis emphasizes the importance of
592 human demography and prior immunity in structuring dengue transmission globally. Consistent
593 with studies conducted elsewhere (23–25), we observed a pattern of increasing mean age of
594 reported dengue infection that we effectively recaptured by modeling a declining FOI through
595 time—which we attributed to declining birth and death rates consistent with Cambodia's

596 demographic transition. Certainly, other mechanisms of demographic change (e.g. immigration
597 and emigration) could also impact infection dynamics. Cambodia experienced a net negative
598 migration rate across the time series investigated (60); as the majority of Cambodian migrants are
599 young adults seeking employment in neighboring Thailand (61), it is possible that their emigration
600 could lower the dengue FOI even further. Though the Cambodian migrant population comprises
601 <0.5% of the total national population (60), migration rates can be 10-fold higher in border
602 provinces and could have correspondingly elevated impacts in these regions (61).

603 The declining FOI through time is somewhat counterintuitive considering recent explosive
604 dengue epidemics in Cambodia and across the globe. Nonetheless, we provide evidence for a
605 high frequency of reported cases in older age individuals that underlies the high case burden in
606 epidemic years. Our study is unique from previous investigations in recognition, not only of
607 escalation of the mean age of reported dengue infection, but also of the expanding age range of
608 reported disease. Indeed, symptomatic individuals >70 years in age during the 2019 epidemic are
609 difficult to reconcile under assumptions by which reported cases correspond to clinically apparent
610 secondary infections only. In our modeling framework, we take a novel approach to account for
611 these infections by allowing for waning multitypic immunity and repeated symptomatic infections
612 in older age individuals.

613 Recent analyses out of the Thailand system highlight a similar uptick in case reports
614 among older individuals (23), which the authors attribute to increased detectability in tertiary and
615 quaternary infections. The authors offer a series of hypothetical explanations for increasing case
616 detectability through time: that tertiary and quaternary dengue infections might be more
617 pathogenic (and therefore more detectable) due to an abundance of comorbidities in older
618 individuals, that immunopathology may be exacerbated in older patients who experienced longer
619 durations between repeat infections; or that waning multitypic immunity could allow for repeat
620 infections in the oldest age cohorts (our hypothesis). Our analyses in the Cambodia system are
621 not mutually exclusive with any of these explanations; however, we hypothesize that, were
622 comorbidities or immunopathogenesis in older individuals driving patterns in the observed data,

623 we would expect to see an hour-glass shape in symptomatic cases, with reduced reporting in
624 middle-aged individuals who have progressed beyond secondary exposures but are at lower risk
625 for both comorbidities and immunopathology. Instead, we see a gradual tapering in the age-
626 frequency of infection, which expands in range with time (Fig. S15), consistent with the
627 hypothesis of waning multitypic immunity. This latter hypothesis, when considered in association
628 with genotype replacement, can also explain isolated expansion and subsequent contraction in
629 the age range of reported cases witnessed in epidemic years, while the first two hypotheses
630 cannot. In addition, hypotheses of heightened pathology in more frequent older age infections are
631 difficult to reconcile in Cambodia with nationally-reported declines in the dengue mortality burden
632 despite increasing caseload through time (15).

633 Our deterministic model simulations demonstrate how short-term spikes in the age
634 distribution of reported cases, independent of the mean annual trend in the time series, can be
635 achieved via introduction of an antigenically distinct lineage (either a divergent genotype within an
636 established serotype, or a novel serotype) into an endemic, 3-serotype system. Though limited in
637 scope, PCR-based sentinel surveillance data provide no support for serotype turnover associated
638 with the 2019 dengue epidemic in Cambodia (15). By contrast, genome sequencing data from our
639 own febrile cohort study offer support for a genotype replacement event. Recent analyses of the
640 Thailand system link transitions in serotype dominance and clade replacement of genotype
641 sublineages within a single serotype to epidemic magnitude (34, 35). In Thailand, the most
642 severe epidemics were linked to clade replacement of a resident viral genotype by an
643 evolutionarily fitter DENV lineage within the same serotype, resulting in a 'selective sweep', which
644 subsequently reduced overall viral diversity and, consequently, diminished between-serotype
645 antigenic differences (34). In the 2019 epidemic in Cambodia, emergence of the Cosmopolitan
646 genotype, followed by serotypic and genotypic homogeneity in 2020-2022, are consistent with the
647 dynamics of clade replacement within DENV-2. Indeed, prior clade replacements have been
648 associated with epidemics in Cambodia (17, 18) and elsewhere (49, 53, 62–64).

649 As one limitation of our study, the bulk of our genotyping efforts were concentrated in
650 peri-urban Kampong Speu province, allowing for the possibility that the clade replacement
651 phenomenon documented here may be regionally localized, with consequentially limited impacts
652 on national caseloads. Nonetheless, the predominance of the DENV-2 Asian 1 lineage in the mid-
653 2000s has been well-documented across most provinces in Cambodia (65, 66), and our extended
654 sequencing efforts in 2021-2022 suggest that the Cosmopolitan takeover covered a similarly
655 widespread geographic extent. Additionally, reemergence of DENV-2 Cosmopolitan lineage has
656 also been documented in neighboring Vietnam and associated with a 2019 epidemic (52),
657 suggesting a more generalized regional phenomenon.

658 Our study faces additional limitations in that we were unable to obtain virus isolates and
659 undertake subsequent antigenic cartography (67), which would be needed to resolve whether the
660 emerging Cosmopolitan genotype in Cambodia is, indeed, antigenically distinct from previously
661 circulating Asian 1 lineages of DENV-2 and, potentially, more antigenically similar to endemic
662 heterotypic viruses. Indeed, because much of our inference is derived from serotype-agnostic
663 national surveillance data, we are unable to rigorously evaluate the role of a possible genotype
664 replacement event in particularly driving a high burden of disease in the oldest-age (>70 years)
665 individuals in NDCP dataset. Nonetheless, the expansion of this lineage following the 2019
666 epidemic offers support for the enhanced fitness of this genotype. In addition, our own febrile
667 surveillance study demonstrates a significantly older mean age of infection for DENV-2
668 Cosmopolitan cases than for DENV-1 cases, which further supports our hypothesis of invasion
669 paired with immune escape. Critically, our simulation analyses demonstrate how the expanded
670 age distribution of cases witnessed across epidemic years in Cambodia can only be recovered
671 under assumptions of lineage-specific immune invasion.

672 Several published studies offer regional explanations for the global dengue phenomenon
673 of 2019. Recent analyses from Brazil, for example, argue that a low FOI in 2017 and 2018
674 resulting from new public health interventions and behavioral modifications implemented in the
675 wake of the Zika virus epidemic drove a resurgence in cases in 2019 and an expansion of

specific lineages of DENV-1 and DENV-2 that had been circulating cryptically for much of the past decade (68). Independent work in the same region indicates that the DENV-2 lineage responsible for the Brazilian outbreak additionally caused a clade replacement event (63). Dengue surged worldwide in 2019, though the factors driving this surge appear to be somewhat heterogenous across ecosystems. Nonetheless, our study lends support for the role of climate in synchronizing epidemic dynamics across landscapes; it is possible that optimal climate conditions may facilitate expansion of low prevalence lineages with intrinsic fitness advantages (e.g. higher replication rate, shorter incubation period (69)) over resident genotypes, thus driving epidemics. Previous modeling studies have suggested that invading dengue lineages may circulate at low prevalence in a host population for many years prior to detection, expansion, and displacement of resident clades in the same serotype (70).

Here, we propose the emergence of the DENV-2 Cosmopolitan genotype, coupled with a subtle climate-driven increase in FOI, and overlaid on the background of an aging population with waning multitypic immunity, as one possible explanation for Cambodia's largest recorded dengue epidemic to date. Our study emphasizes the extraordinary dearth of publicly available DENV sequence data for SEA; indeed, DENV is sequenced so infrequently in Cambodia that it is impossible to know whether 2019 truly marked the first year of DENV-2 Cosmopolitan introduction to the country, or simply the year of intensified expansion and consequential epidemic dynamics. More broadly, our work illustrates the importance of the combined forces of climate, demography, immunology, and virology in driving increasingly severe dengue epidemics. As the global burden of dengue continues to expand, ongoing serological and genomic surveillance is needed to improve epidemic forecasting in Southeast Asia and around the world.

METHODS

Data

Detailed descriptions of NDCP case data, climate data, and Kampong Speu febrile surveillance data used in these analyses are reported in the *SI Appendix.*

Climate analyses

We used GAMs to quantify intra- and interannual trends and identify any years that might be considered climatic anomalies, defined as a statistically significant partial effect of a single year on the long-term time series for temperature and precipitation (Fig. S1-4; Table S1; *SI Appendix*). In addition, we reduced temperature and precipitation time series by province into z-scores for visualization (Fig. S5-6).

Climate-informed TSIR modeling

Using the R package tSIR (42), we fit time series Susceptible-Infected-Recovered models (42–44) to the province level dengue data for the three inter-epidemic periods (2002-2006, 2008-2011, and 2013-2018), compiled at biweekly intervals corresponding to the generation time of the pathogen (*SI Appendix*). Using TSIR transmission parameters, we projected cases in subsequent epidemic years (2007, 2012, 2019) by province. We then followed Wagner et al. 2020 (49) to estimate the factorial increase in reconstructed susceptible population needed to recover case counts for the three epidemic years.

We next used cross correlation analysis to determine the optimal lag between biweekly mean temperature and total precipitation versus transmission at the province level; we estimated a median 3.5 month lag for temperature and 1 month lag for precipitation, consistent with prior analyses (Table S3; *SI Appendix*) (49). We then constructed a suite of regression models (including GAMs) for each interepidemic period, incorporating a response variable of the log of biweekly transmission with the corresponding predictors of optimally lagged biweekly mean

730 temperature and total precipitation per province (45, 49) (Fig. S8-10; Table S4). We used lagged
731 temperature and precipitation from each epidemic year in each province in a fitted GAM to project
732 climate-informed transmission rates for 2007, 2012, and 2019 (*SI Appendix*). We then simulated
733 TSIR using climate-informed transmission rates to recover epidemic year predictions of province-
734 level caseload. Because climate-derived transmission rates still failed to recover epidemic peaks,
735 we allowed another susceptible amplification term to determine the relative increase in
736 susceptible population needed to recover epidemic dynamics even after accounting for climate
737 (Table S5).
738
739 *Wavelet analyses*
740 We next used wavelet decomposition in the R package 'WaveletComp' (50) to explore
741 annual and multiannual periodicity in dengue epidemics and climate variables. We converted
742 biweekly case totals by province from the NDCP data into incidence rates per 100,000
743 population, then used a Morlet wavelet with nondimensional frequency ($\omega = 6$) to extract,
744 detrend, and reconstruct annual cycles in dengue incidence with a maximum period of two years
745 and multiannual cycles with periods ranging from two to 20 years (Fig. 2AB) (28, 29). We
746 additionally calculated the average wavelet power (squared amplitude, here averaged across all
747 significant wavelets within a specified timestep) for significant cycles within each biweekly
748 timestep for annual and multiannual cycles per province (Fig. S11AB).
749 We investigated synchronicity in dengue incidence across space by computing the
750 Pearson's correlation coefficient (ρ) and the mean cross-wavelet power spectrum between
751 province pairs, using the annual raw incidence and reconstructed annual and multiannual cycles
752 (the latter averaged over a sliding 5-year interval) (Fig. 2CD, S11CD; *SI Appendix*). We
753 constructed a GAM to identify statistical correlates of high synchronicity pairs (Fig. S12; Table S6;
754 *SI Appendix*). To investigate synchrony between dengue and climate, we computed mean cross-
755 wavelet power between biweekly dengue incidence and mean temperature (Fig. S13A) and total
756 precipitation (Fig. S13B) per province, then repeated between reconstructed multiannual dengue

757 cycles over a 5-year interval and the same two climate variables, again per province (Fig.
758 S13CD). Finally, we reconstructed *monthly* multiannual dengue cycles per province to compute
759 average cross-wavelet power with the Oceanic Niño Index (ONI), a time series quantifying the
760 intensity of the El Niño Southern Oscillation (Fig. S13E). Lastly, we extracted the mean period
761 from reconstructed multiannual dengue cycles by province and nationally, to compare with
762 demographic data (birth rates, death rates, population size (60)) (Fig. S14).
763
764 *Increasing age of reported infection and FOI estimation*
765 To quantify interannual trends in the mean age of reported DENV infection, we fit a GAM
766 with a response variable of age to a fixed predictor of the interaction of year and province, with a
767 random effect of province, allowing both slope and y-intercept to vary by locality. We visualized
768 trends across the age distribution of reported cases by province (Fig. S15) and summarized
769 nationally (Fig. 3AB; Table S7).
770 To estimate annual FOI for DENV in Cambodia from 2002-2020, we applied the model
771 developed by Ferguson et al. 1999 (36) and Cummings et al. 2009 (24) to age-structured
772 incidence recovered from the NDCP data, at the province level, assuming reported cases to
773 represent secondary infections and individuals in the dataset to experience exposure to multiple
774 DENV serotypes across their lifetimes. We allowed for a unique FOI across each year in the time
775 series but first assumed constant FOI across all age cohorts within a year. We estimated one FOI
776 per year per province (excepting Tboung Khmum), in addition to a summary national FOI, for all
777 years in the dataset and extending back to the year of birth for the oldest individual in the first
778 year of the corresponding data subset (40 years for national data) (Fig. S16; Table S8; *SI*
779 *Appendix*). We estimated mean FOI per serotype assuming four circulating dengue serotypes
780 and plotted FOI estimates in comparison to national reported birth and death rates (Fig. 3C) (60).
781 After fixing FOI by province, we followed prior work (24) to estimate FOI modifiers by age,
782 shared across all provinces. We fit nineteen age-specific modifiers to the fixed FOI values,
783 corresponding to eight age classes in first decade of the dataset and eleven in the second

784 decade, where the age distribution was larger (Table S8). We then modified our model to allow
785 waning from multitypic back to monotypic immunity (σ), such that older individuals could
786 experience renewed symptomatic infections (*SI Appendix*). As with age-modification terms, we
787 estimated waning multitypic immunity shared across all provinces but allowed σ to vary annually.
788 We compared fits of FOI-only, FOI with age modification, FOI with waning multitypic immunity,
789 and FOI with both age modification and waning multitypic immunity models to the data (Table
790 S8), then simulated the resulting accumulation of cases with age from the best fit model at
791 national (Fig. 3E) and province levels (Fig. S17).
792
793 *Viral sequencing*
794 mNGS was applied to RNA extracted from 239 serum samples collected from patients
795 reporting with symptoms in our 2019-2022 febrile cohort study in Kampong Speu province, with
796 an additional subset of 11 samples sourced from five nearby provinces (39). A further 20 samples
797 were received for RNA extraction and mNGS from six provinces (including 8 from Kampong
798 Speu) in part with 2021-2022 NDCP surveillance (Table S9; Fig. 4AB). See *SI Appendix* for
799 detailed methods for library preparation, sequencing, and consensus genome generation. We
800 successfully generated 192 full or near-full genome sequences from the original 270 samples,
801 which we submitted to NCBI (63 DENV-1, 120 DENV-2, and 9 DENV-4). All contributed genomes
802 were >10,000 bps in length and had a maximum of 90 Ns (corresponding to <1% of the DENV
803 genome). Samples for which full genome recovery was not possible were identified to genotype
804 using BLAST (71) and visualized in Fig. 4AB (Table S9).
805
806 *Phylodynamic and phylogenetic analysis*
807 See *SI Appendix* for details of sequence selection for Bayesian phylodynamic timetrees
808 and maximum likelihood phylogenies. After selection, sequences were aligned by serotype in the
809 program MAFFT (72), and the best fit nucleotide substitution model for each serotype was
810 evaluated in ModelTest-NG (73). Using the best-fit model (GTR+I+G4 in all cases), we built a

811 Bayesian phylogenetic tree for each serotype in BEAST 2 (56), incorporating the date of sample
812 collection for each sequence (or the midpoint of the collection year if date was not reported), and
813 specifying a strict molecular clock rate of 7.9×10^{-4} s/s/y (8) and a Coalescent Bayesian skyline
814 prior. We ran Markov Chain Monte Carlo chains for 150 million iterations, logging results every
815 10,000 iterations. After chains completed, we removed the initial 10% of iterations as burn-in and
816 evaluated parameter convergence (ESS$\geq$ 200) in Tracer v1.6. We summarized resulting
817 phylogenetic trees in TreeAnnotator and visualized summary trees in ggtree (74) (Fig. 4CD; Fig.
818 S18, S19). Serotype-specific maximum likelihood phylogenetic trees were constructed in RAxML
819 (75). Twenty ML inferences were made on each original alignment and bootstrap replicate trees
820 were inferred using Felsenstein's method (76), with the MRE-based bootstopping test applied
821 after every 50 replicates (77). Resulting phylogenies were visualized in ggtree (74) (Fig. S18).
822 We followed Salje et al. 2017 (8) to calculate the proportion of sequences within each
823 DENV serotype that could be attributed to the same transmission chain on our Bayesian
824 timetrees, defined as having an MRCA within the past six months in the same season (see Fig.
825 S20 for alternative MRCA cutoffs). We compared the proportion of DENV-1 vs. DENV-2
826 sequences sharing a transmission chain to the Euclidean distance separating the GPS
827 coordinates for each sequence pair (Fig. 4E). We then computed the total effective number of
828 transmission chains (the reciprocal of the proportion of sequences sharing a chain) in our 2019-
829 2022 Kampong Speu sequence dataset for DENV-1 and DENV-2 at the World Bank reported
830 population density for Kampong Speu province (60) (Fig. 4F).
831
832 *Mechanistic modeling of age-structured dengue dynamics*
833 Finally, we constructed a mechanistic, age-structured discrete time deterministic model in
834 biweekly timesteps (57–59) to simulate three-serotype dengue dynamics in a population
835 demographically structured to mimic that of Cambodia over the past half-century (*SI Appendix*).
836 We compared simulations under (H0) baseline demographic assumptions with simulations of (H1)
837 increasing tertiary case detections through time and (H2) genotype invasion and clade-

replacement with waning immunity, timed both in 2019 and in 2007. We additionally simulated novel genotype invasions under (H3) assumptions of no antigenic escape, or (H4) lineage-agnostic increasing tertiary case detection (Fig. S21). Finally, we fit the Ferguson-Cummings four-serotype catalytic model to the simulated data for each hypothesis to recapture the input FOI (Fig. S22). Holding FOI constant, we estimated a time-varying signature of waning monotypic immunity for all simulated time series (Fig. S22).

ACKNOWLEDGEMENTS

This research is supported by the Division of Intramural Research at the National Institute of Allergy and Infectious Diseases at the National Institutes of Health and the Bill and Melinda Gates Foundation [OPP1211806, OPP1211841]. We thank patients and families of Kampong Speu District Referral Hospital who participated in this study, members of the National Dengue Control Program not listed in the author byline, and the Provincial Health Department of Kampong Speu province in Cambodia. We thank Brian Moyer and the NIAID Office of Cyberinfrastructure and Computational Biology (OCICB) for assistance in improving the cyberinfrastructure of our Cambodian field sites. We thank employees at the Chan Zuckerberg Biohub and Chan Zuckerberg Initiative not listed in the author byline. This work was completed with resources provided by the University of Chicago Research Computing Center.

865 **REFERENCES**

866 1. World Health Organization, Dengue and severe dengue. *WHO Fact Sheets* (2022).

867 2. S. Bhatt, *et al.*, The global distribution and burden of dengue. *Nature* **496**, 504–507 (2013).

868 3. A. B. Sabin, Research on dengue during World War II. *American Journal of Tropical*
869 *Medicine and Hygiene* **1**, 30–50 (1952).

870 4. L. C. Katzelnick, *et al.*, Antibody-dependent enhancement of severe dengue disease in
871 humans. *Science (New York, N.Y.)* **932**, 929–932 (2017).

872 5. L. C. Katzelnick, *et al.*, Zika virus infection enhances future risk of severe dengue disease.
873 *Science* **369**, 1123–1128 (2020).

874 6. T. N. Peng, "Southeast Asia's demographic situation, regional variations, and national
875 challenges" in D. Singh, M. Cook, Eds. (ISEAS Publishing, 2017), pp. 55–82.

876 7. G. W. Jones, "The Population of Southeast Asia" (2013).

877 8. H. Salje, *et al.*, Dengue diversity across spatial and temporal scales: Local structure and the
878 effect of host population size. *Science (New York, N.Y.)* **355**, 1302–1306 (2017).

879 9. statista, Cambodia: Urbanization from 2010 to 2020.
880 *https://www.statista.com/statistics/455789/urbanization-in-cambodia/.* (2022).

881 10. J. H. Huber, M. L. Childs, J. M. Caldwell, E. A. Mordecai, Seasonal temperature variation
882 influences climate suitability for dengue, chikungunya, and Zika transmission. *PLoS Negl*
883 *Trop Dis* **12**, e0006451 (2018).

884 11. E. A. Gould, S. Higgs, Impact of climate change and other factors on emerging arbovirus
885 diseases. *Transactions of the Royal Society of Tropical Medicine and Hygiene* **103**, 109–121
886 (2009).

887 12. J. P. Messina, *et al.*, The current and future global distribution and population at risk of
888 dengue. *Nature Microbiology* **4**, 1508–1515 (2019).

889 13. Hahn, H., Chastel, C., Dengue in Cambodia in 1963. Nineteen laboratory-proved cases.
890 *American Journal of Tropical Medecine and Hygiene* **19**, 106–109 (1970).

891 14. R. Huy, *et al.*, National dengue surveillance in Cambodia 1980–2008: epidemiological and
892 virological trends and the impact of vector control. *Bull. World Health Organ.* **88**, 650–657
893 (2010).

894 15. C. Yek, *et al.*, National dengue surveillance, Cambodia 2002–2020. *Bull World Health Org*
895 **101**, 605–616 (2023).

896 16. D. S. Burke, A. Nisalak, D. E. Johnson, A prospective study of dengue infections in Bangkok.
897 *The American Journal of Tropical Medicine and Hygiene* **38**, 172–180 (1988).

898 17. V. Duong, *et al.*, Genetic diversity and lineage dynamic of dengue virus serotype 1 (DENV-
899 1) in Cambodia. *Infection, Genetics and Evolution* **15**, 59–68 (2013).

900 18. O. O'Connor, *et al.*, Potential role of vector-mediated natural selection in dengue virus
901 genotype/lineage replacements in two epidemiologically contrasted settings. *Emerging*
902 *Microbes and Infections* **10**, 1346–1357 (2021).

903 19. A. A. Lover, *et al.*, Spatial epidemiology and climatic predictors of paediatric dengue
904 infections captured via sentinel site surveillance, Phnom Penh Cambodia 2011-2012. *BMC*
905 *Public Health* **14** (2014).

906 20. Y. Arima, M. Chiew, T. Matsui, Epidemiological update on the dengue situation in the
907 Western Pacific Region, 2012. *Western Pacific surveillance and response journal : WPSAR*
908 **6**, 82–89 (2015).

909 21. S. Ly, *et al.*, Asymptomatic dengue virus infections, Cambodia, 2012–2013. *Emerging*
910 *Infectious Diseases* **25**, 1354–1362 (2019).

911 22. S. Vong, *et al.*, Under-recognition and reporting of dengue in Cambodia: A capture-
912 recapture analysis of the National Dengue Surveillance System. *Epidemiology and Infection*
913 **140**, 491–499 (2012).

914 23. A. T. Huang, *et al.*, Assessing the role of multiple mechanisms increasing the age of dengue
915 cases in Thailand. *Proc. Natl. Acad. Sci. U.S.A.* **119**, e2115790119 (2022).

916 24. D. A. T. Cummings, *et al.*, The impact of the demographic transition on dengue in Thailand:
917 Insights from a statistical analysis and mathematical modeling. *PLoS Medicine* **6** (2009).

918 25. L. C. Katzelnick, *et al.*, Dynamics and determinants of the force of infection of dengue virus
919 from 1994 to 2015 in Managua, Nicaragua. *Proceedings of the National Academy of*
920 *Sciences of the United States of America* **115**, 10762–10767 (2018).

921 26. N. Ferguson, R. Anderson, S. Gupta, The effect of antibody-dependent enhancement on
922 the transmission dynamics and persistence of multiple-strain pathogens. *Proc. Natl. Acad.*
923 *Sci. U.S.A.* **96**, 790–794 (1999).

924 27. S. I. Hay, *et al.*, Etiology of interepidemic periods of mosquito-borne disease. *Proc. Natl.*
925 *Acad. Sci. U.S.A.* **97**, 9335–9339 (2000).

926 28. B. García-Carreras, *et al.*, Periodic synchronisation of dengue epidemics in Thailand over
927 the last 5 decades driven by temperature and immunity. *PLoS Biol* **20**, e3001160 (2022).

928 29. W. G. van Panhuis, *et al.*, Region-wide synchrony and traveling waves of dengue across
929 eight countries in Southeast Asia. *Proc. Natl. Acad. Sci. U.S.A.* **112**, 13069–13074 (2015).

30. D. A. T. Cummings, I. B. Schwartz, L. Billings, L. B. Shaw, D. S. Burke, Dynamic effects of antibody-dependent enhancement on the fitness of viruses. *Proceedings of the National Academy of Sciences* **102**, 15259–15264 (2005).

31. K. L. McElroy, *et al.*, Endurance, refuge, and reemergence of dengue virus type 2, Puerto Rico, 1986–2007. *Emerg. Infect. Dis.* **17**, 64–71 (2011).

32. B. Adams, *et al.*, Cross-protective immunity can account for the alternating epidemic pattern of dengue virus serotypes circulating in Bangkok. *Proceedings of the National Academy of Sciences of the United States of America* **103**, 14234–9 (2006).

33. C. V. F. Carrington, J. E. Foster, O. G. Pybus, S. N. Bennett, E. C. Holmes, Invasion and maintenance of Dengue virus type 2 and type 4 in the Americas. *Journal of Virology* **79**, 14680–14687 (2005).

34. L. C. Katzelnick, *et al.*, Antigenic evolution of dengue viruses over 20 years. *Science* (2021).

35. S. M. Bell, L. Katzelnick, T. Bedford, Dengue genetic divergence generates within-serotype antigenic variation, but serotypes dominate evolutionary dynamics. *eLife* **8**, e42496 (2019).

36. N. M. Ferguson, C. A. Donnelly, R. M. Anderson, Transmission dynamics and epidemiology of dengue: insights from age-stratied sero-prevalence surveys. *Proceedings of the Royal Society B* **354**, 757–768 (1999).

37. Hugo. Muench, *Catalytic models in epidemiology.* (Harvard University Press, 1959).

38. J. E. Manning, *et al.*, Development of inapparent dengue associated with increased antibody levels to *Aedes aegypti* salivary proteins: A longitudinal dengue cohort in Cambodia. *The Journal of Infectious Diseases* (2021). https://doi.org/10.1093/infdis/jiab541.

39. J. A. Bohl, *et al.*, Discovering disease-causing pathogens in resource-scarce Southeast Asia using a global metagenomic pathogen monitoring system. *Proceedings of the National Academy of Sciences* **119**, e2115285119 (2022).

40. S. N. Wood, mgcv: GAMs and Generalized Ridge Regression for R. *R News* **1/2**, 20–24 (2001).

41. NOAA: National Weather Service, *Climate Predication Scenter: Cold & Warm Episodes by Season* (2023). Available at: https://origin.cpc.ncep.noaa.gov/products/analysis_monitoring/ensostuff/ONI_v5.php.

42. A. D. Becker, B. T. Grenfell, TSIR: An R package for time-series susceptible-infected-recovered models of epidemics. *PLoS ONE* **12**, 1–10 (2017).

43. O. N. Bjornstad, B. F. Finkenstadt, B. T. Grenfell, Dynamics of measles epidemics: Estimating scaling of transmission rates using a times series SIR model. *Ecological Monographs* **72**, 169–184 (2002).

44. B. T. Grenfell, O. N. Bjornstad, B. F. Finkenstadt, Dynamics of measles epidemics: Scaling noise, determinism, and predictability with the TSIR Model. *Ecological Monographs* **72**, 185–202 (2002).

45. R. J. Oidtman, *et al.*, Inter-annual variation in seasonal dengue epidemics driven by multiple interacting factors in Guangzhou, China. *Nature Communications* **10** (2019).

46. N. A. Rehman, *et al.*, Quantifying the localized relationship between vector containment activities and dengue incidence in a real-world setting: A spatial and time series modelling analysis based on geo-located data from Pakistan. *PLoS Neglected Tropical Diseases* **14**, 1–22 (2020).

47. M. U. G. Kraemer, *et al.*, Big city, small world: density, contact rates, and transmission of dengue across Pakistan. *J. R. Soc. Interface.* **12**, 20150468 (2015).

48. M. U. G. Kraemer, *et al.*, Inferences about spatiotemporal variation in dengue virus transmission are sensitive to assumptions about human mobility: a case study using geolocated tweets from Lahore, Pakistan. *EPJ Data Science* **7** (2018).

49. C. E. Wagner, *et al.*, Climatological, virological and sociological drivers of current and projected dengue fever outbreak dynamics in Sri Lanka. *Journal of the Royal Society Interface* **17** (2020).

50. Roesch, Angi, Schmidbauer, Harald, WaveletComp: Computational Wavelet Analysis. R package version 1.1. (2018). Deposited 2018.

51. J. Phadungsombat, *et al.*, Emergence of genotype cosmopolitan of dengue virus type 2 and genotype III of dengue virus type 3 in Thailand. *PLoS ONE* **13**, 1–26 (2018).

52. V. T. Tran, *et al.*, Reemergence of Cosmopolitan genotype dengue virus serotype 2, southern Vietnam. *Emerg. Infect. Dis.* **29** (2023).

53. A. Wijewickrama, *et al.*, Emergence of a Dengue virus serotype 2 causing the largest ever dengue epidemic in Sri Lanka. *bioRxiv* (2018). https://doi.org/10.1101/329318.

54. H. A. Tissera, *et al.*, Severe dengue epidemic, Sri Lanka, 2017. *Emerg. Infect. Dis.* **26**, 682–691 (2020).

55. A. J. Drummond, M. A. Suchard, D. Xie, A. Rambaut, Bayesian phylogenetics with BEAUti and the BEAST 1.7. *Molecular Biology and Evolution* **29**, 1969–1973 (2012).

56. R. Bouckaert, *et al.*, BEAST 2: A software platform for Bayesian evolutionary analysis. *PLoS Computational Biology* **10** (2014).

57. P. Klepac, H. Caswell, The stage-structured epidemic: Linking disease and demography with a multi-state matrix approach model. *Theoretical Ecology* **4**, 301–319 (2011).

998 58. C. J. E. Metcalf, *et al.*, Structured models of infectious disease: Inference with discrete
999 data. *Theoretical Population Biology* **82**, 275–282 (2012).

1000 59. P. Klepac, *et al.*, Stage-structured transmission of phocine distemper virus in the Dutch
1001 2002 outbreak. *Proceedings. Biological sciences / The Royal Society* **276**, 2469–2476
1002 (2009).

1003 60. World Bank, Cambodia. *World Development Indicators* (2021). Available at:
1004 https://data.worldbank.org/country/KH [Accessed 12 April 2022].

1005 61. I. A. Sampson, G. M. Miles, E. Piano, "Undocumented, unregistered and invisible": an
1006 exploratory study of the reasons for and effects of migrating to Thailand of Cambodian
1007 young people. *IJSSP* **41**, 862–874 (2021).

1008 62. L. Lambrechts, *et al.*, Dengue-1 virus clade replacement in Thailand associated with
1009 enhanced mosquito transmission. *Journal of Virology* **86**, 1853–1861 (2012).

1010 63. J. G. de Jesus, *et al.*, Genomic detection of a virus lineage replacement event of dengue
1011 virus serotype 2 in Brazil, 2019. *Memorias do Instituto Oswaldo Cruz* **115** (2020).

1012 64. K. Suzuki, *et al.*, Genotype replacement of dengue virus type 3 and clade replacement of
1013 dengue virus type 2 genotype Cosmopolitan in Dhaka, Bangladesh in 2017. *Infection,*
1014 *Genetics and Evolution* **75** (2019).

1015 65. V. Duong, *et al.*, Complex dynamic of dengue virus serotypes 2 and 3 in Cambodia
1016 following series of climate disasters. *Infection, Genetics and Evolution* **15**, 77–86 (2013).

1017 66. V. T. T. Hang, *et al.*, Emergence of the Asian 1 genotype of dengue Virus serotype 2 in Viet
1018 Nam: *In Vivo* fitness advantage and lineage replacement in South-East Asia. *PLoS*
1019 *Neglected Tropical Diseases* **4** (2010).

1020 67. L. C. Katzelnick, *et al.*, Dengue viruses cluster antigenically but not as discrete serotypes.
1021 *Science* **349**, 1338–1343 (2015).

1022 68. A. F. Brito, *et al.*, Lying in wait: the resurgence of dengue virus after the Zika epidemic in
1023 Brazil. *Nature Communications* **12**, 1–13 (2021).

1024 69. R. Rico-Hesse, *et al.*, Origins of Dengue type 2 viruses associated with increased
1025 pathogenicity in the Americas. *Virology* **230**, 244–251 (1997).

1026 70. J. Lourenço, M. Recker, Viral and epidemiological determinants of the invasion dynamics of
1027 Novel Dengue Genotypes. *PLoS Neglected Tropical Diseases* **4** (2010).

1028 71. S. F. Altschul, W. Gish, W. Miller, E. W. Myers, D. J. Lipman, Basic local alignment search
1029 tool. *Journal of Molecular Biology* **215**, 403–410 (1990).

1030 72. K. Katoh, J. Rozewicki, K. D. Yamada, MAFFT online service: Multiple sequence alignment,
1031 interactive sequence choice and visualization. *Briefings in Bioinformatics* **20**, 1160–1166
1032 (2018).

1033 73. Di. Darriba, *et al.*, ModelTest-NG: A new and scalable tool for the selection of DNA and
1034 protein evolutionary models. *Molecular Biology and Evolution* **37**, 291–294 (2020).

1035 74. G. Yu, D. K. Smith, H. Zhu, Y. Guan, T. T. Y. Lam, Ggtree: an R Package for visualization and
1036 annotation of phylogenetic trees with their covariates and other associated data. *Methods*
1037 *in Ecology and Evolution* **8**, 28–36 (2017).

1038 75. A. M. Kozlov, D. Darriba, T. Flouri, B. Morel, A. Stamatakis, RAxML-NG: A fast, scalable and
1039 user-friendly tool for maximum likelihood phylogenetic inference. *Bioinformatics* **35**,
1040 4453–4455 (2019).

1041 76. J. Felsenstein, Confidence limits on phylogenies: An approach using the bootstrap.
1042 *Evolution* **39**, 783–791 (1985).

1043 77. N. D. Pattengale, M. Alipour, O. R. P. Bininda-Emonds, B. M. E. Moret, A. Stamatakis, How
1044 many bootstrap replicates are necessary? *Journal of Computational Biology* **17**, 337–354
1045 (2010).

1046

1047

1048

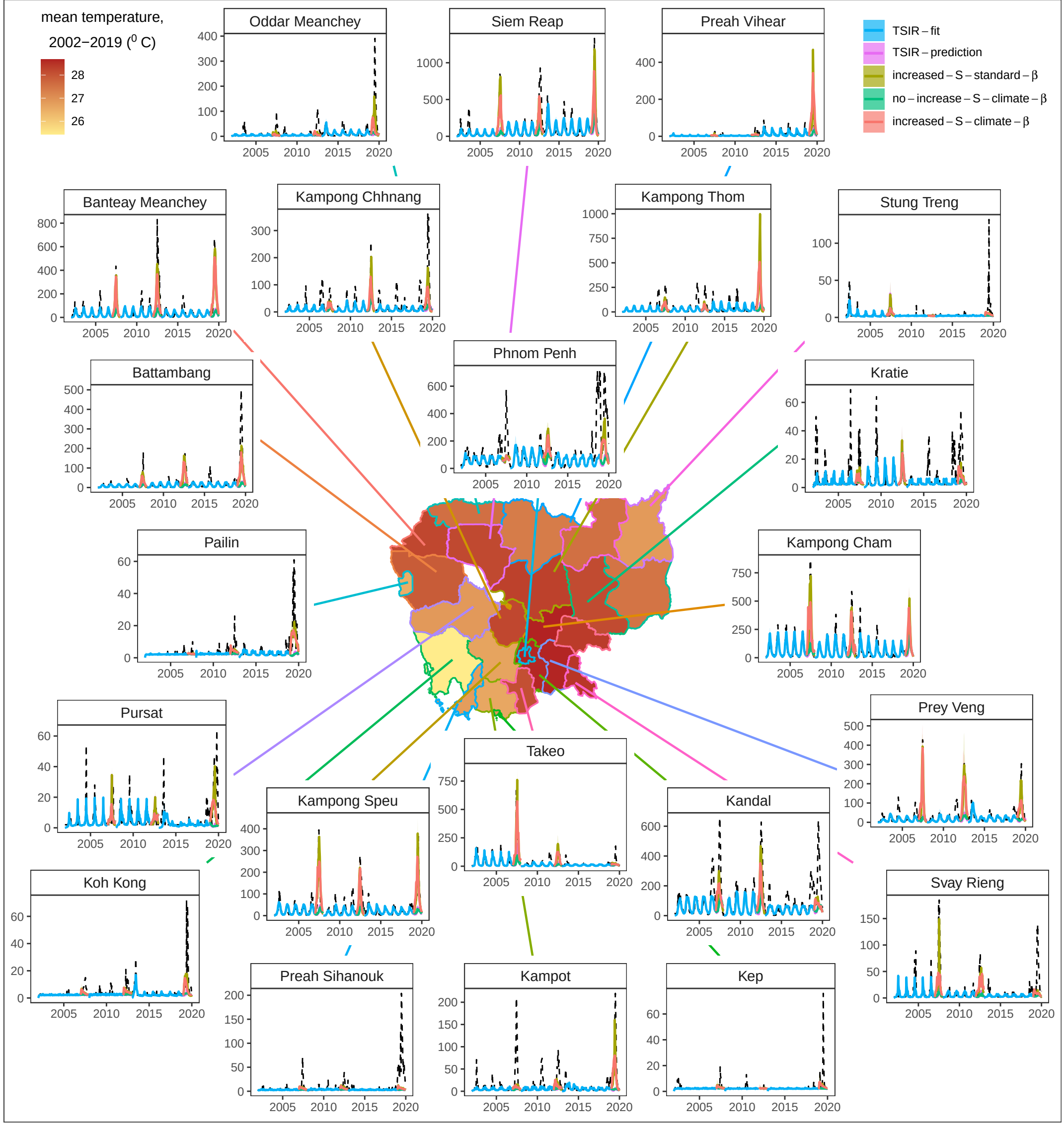
mean temperature,
2002−2019 (0 C)
28
27
26
TSIR – fit
TSIR – prediction
increased – S – standard – β
no – increase – S – climate – β
increased – S – climate – β
Oddar Meanchey
Siem Reap
Preah Vihear
Banteay Meanchey
Kampong Chhnang
Kampong Thom
Stung Treng
Phnom Penh
Battambang
Kratie
Pailin
Kampong Cham
Pursat
Prey Veng
Takeo
Kampong Speu
Kandal
Koh Kong
Svay Rieng
Preah Sihanouk
Kampot
Kep
2005
2010
2015
2020

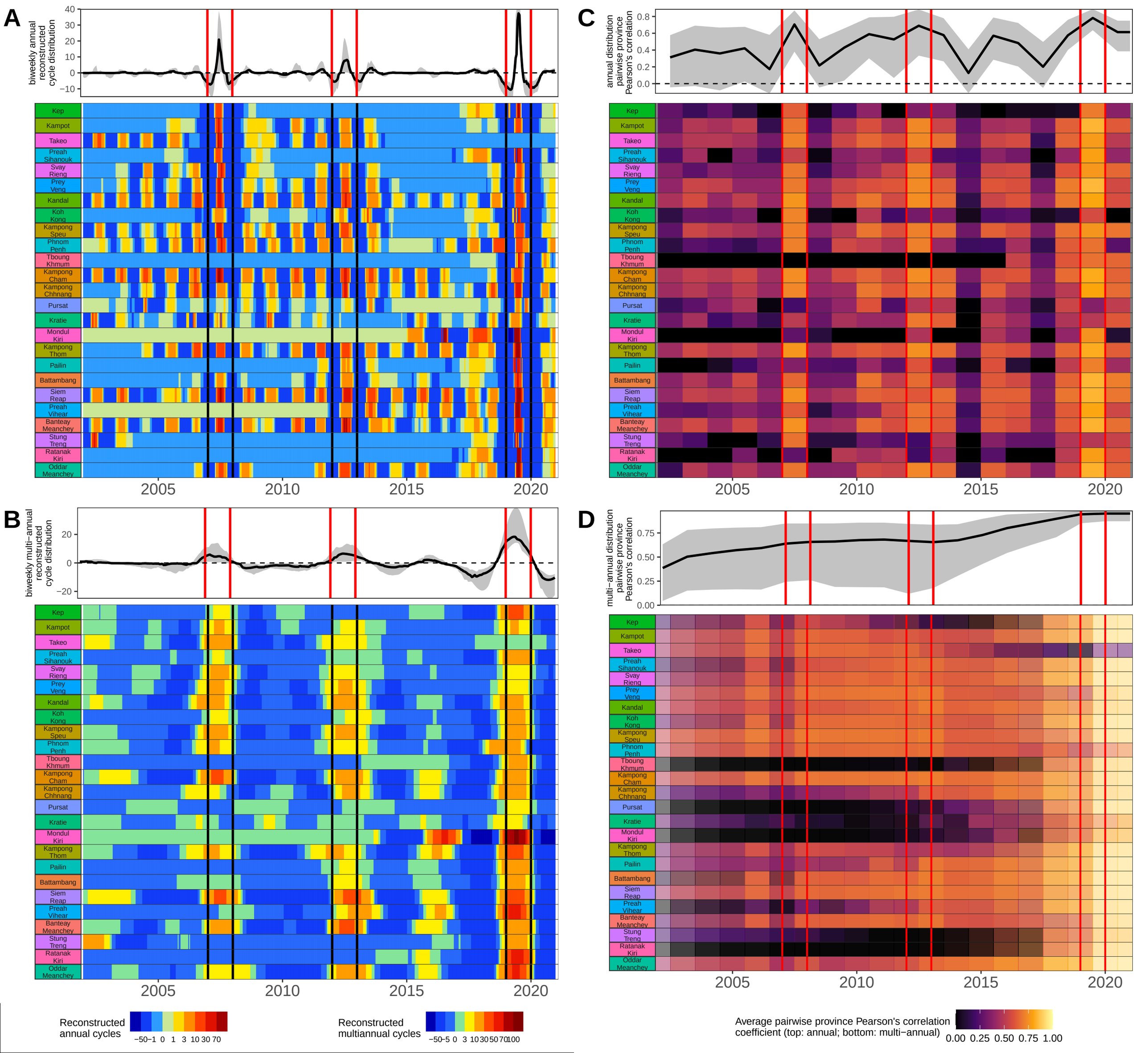
A
biweekly annual reconstructed cycle distribution
40
30
20
10
0
−10
B
biweekly multi−annual reconstructed cycle distribution
20
0
−20
C
annual distribution pairwise province Pearson's correlation
0.8
0.6
0.4
0.2
0.0
D
multi−annual distribution pairwise province Pearson's correlation
0.75
0.50
0.25
0.00
Kep
Kampot
Takeo
Preah Sihanouk
Svay Rieng
Prey Veng
Kandal
Koh Kong
Kampong Speu
Phnom Penh
Tboung Khmum
Kampong Cham
Kampong Chhnang
Pursat
Kratie
Mondul Kiri
Kampong Thom
Pailin
Battambang
Siem Reap
Preah Vihear
Banteay Meanchey
Stung Treng
Ratanak Kiri
Oddar Meanchey
2005
2010
2015
2020
Reconstructed annual cycles
−50 −1 0 1 3 10 30 70
Reconstructed multiannual cycles
−50 −5 0 3 10 30 50 70 100
Average pairwise province Pearson's correlation coefficient (top: annual; bottom: multi−annual)
0.00 0.25 0.50 0.75 1.00

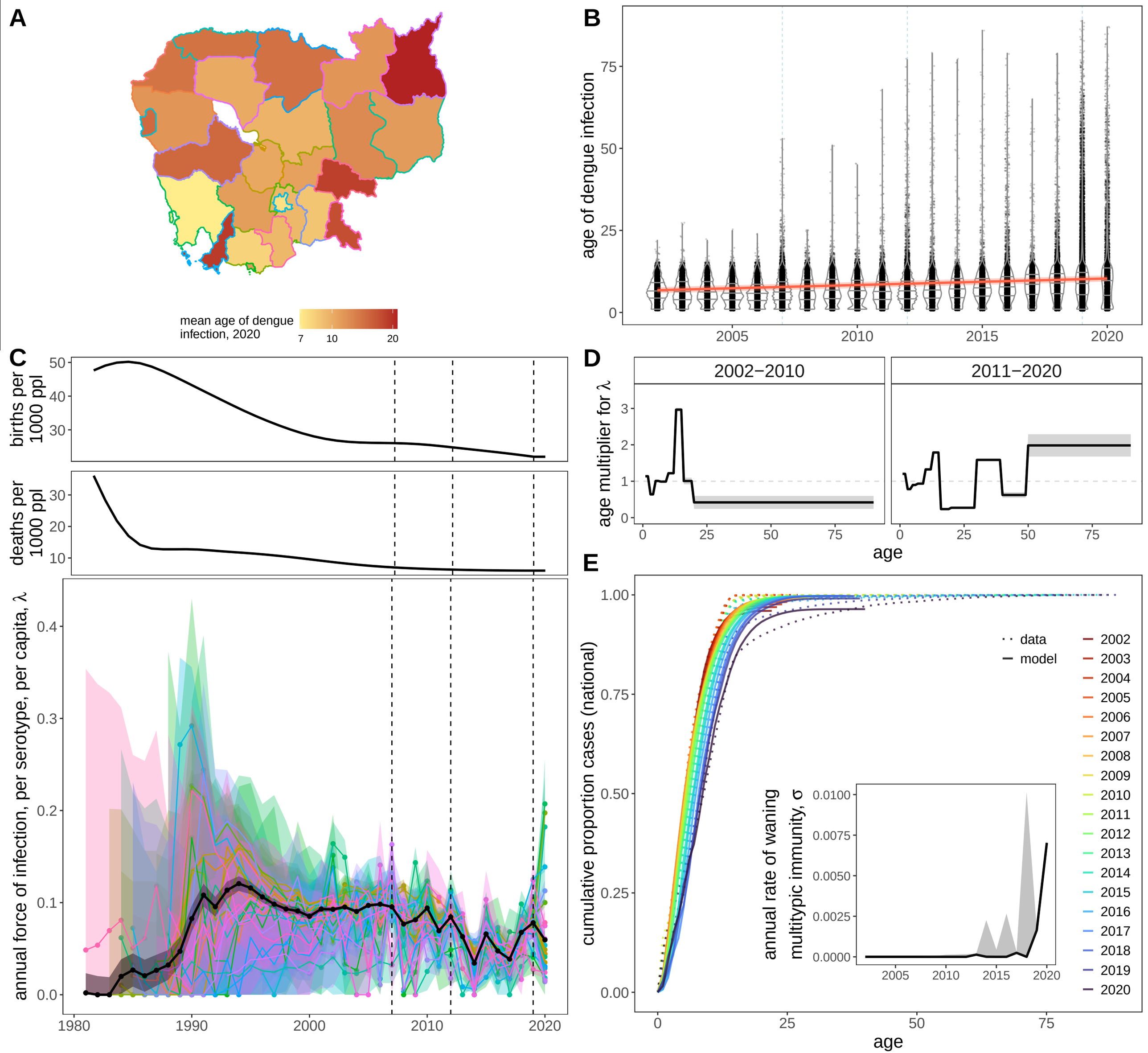
A
mean age of dengue infection, 2020
7
10
20
B
age of dengue infection
0
25
50
75
2005
2010
2015
2020
C
births per 1000 ppl
50
40
30
deaths per 1000 ppl
30
20
10
annual force of infection, per serotype, per capita, λ
0.0
0.1
0.2
0.3
0.4
1980
1990
2000
2010
2020
D
2002−2010
2011−2020
age multiplier for λ
0
1
2
3
0
25
50
75
age
E
cumulative proportion cases (national)
0.00
0.25
0.50
0.75
1.00
data
model
2002
2003
2004
2005
2006
2007
2008
2009
2010
2011
2012
2013
2014
2015
2016
2017
2018
2019
2020
annual rate of waning multitypic immunity, σ
0.0000
0.0025
0.0050
0.0075
0.0100
2005
2010
2015
2020
0
25
50
75
age

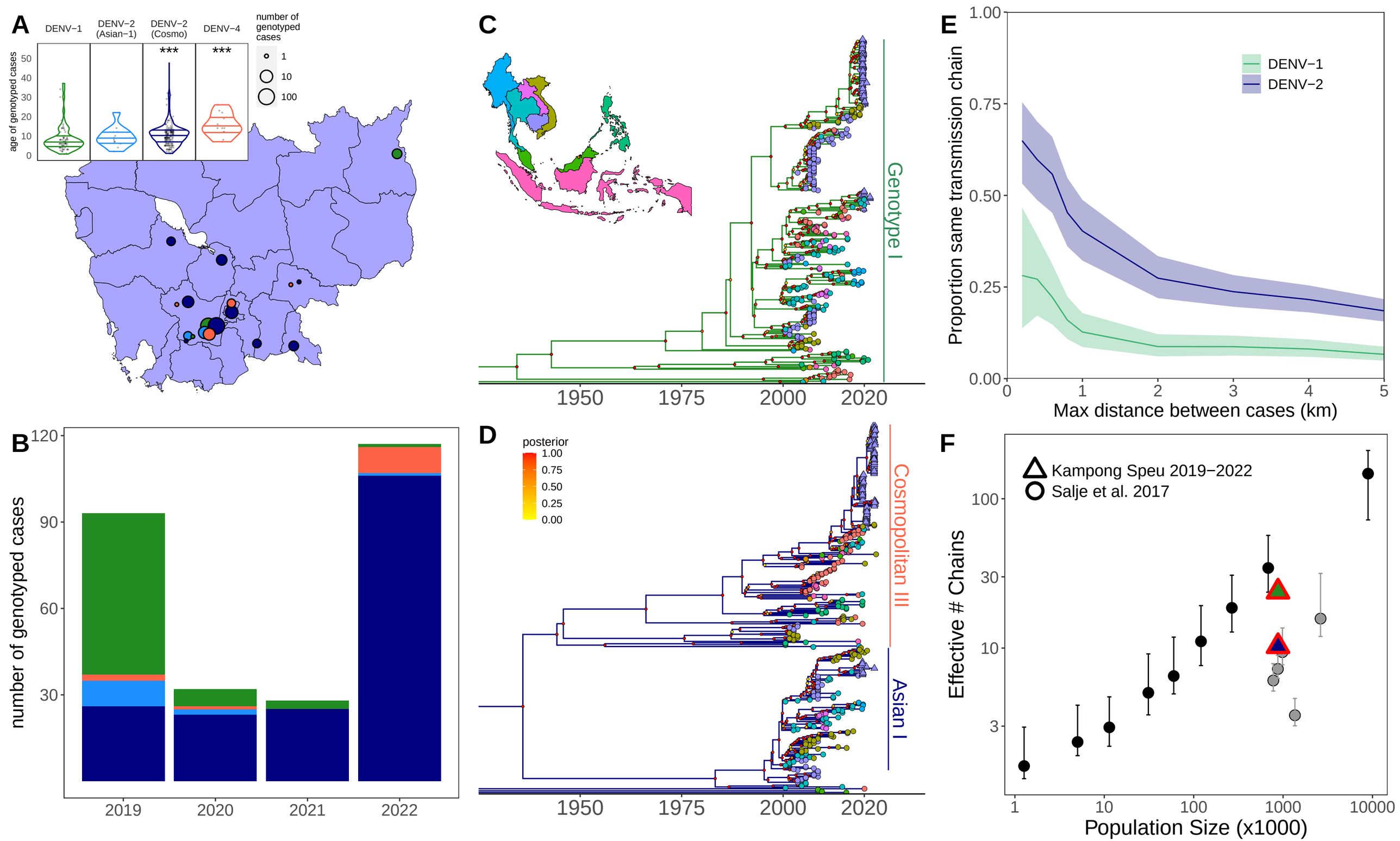
A
DENV−1
DENV−2 (Asian−1)
DENV−2 (Cosmo)
DENV−4
number of genotyped cases
1
10
100
age of genotyped cases
***
***
B
number of genotyped cases
2019
2020
2021
2022
C
Genotype I
1950
1975
2000
2020
D
posterior
1.00
0.75
0.50
0.25
0.00
Cosmopolitan III
Asian I
1950
1975
2000
2020
E
Proportion same transmission chain
DENV−1
DENV−2
Max distance between cases (km)
F
Kampong Speu 2019−2022
Salje et al. 2017
Effective # Chains
Population Size (x1000)

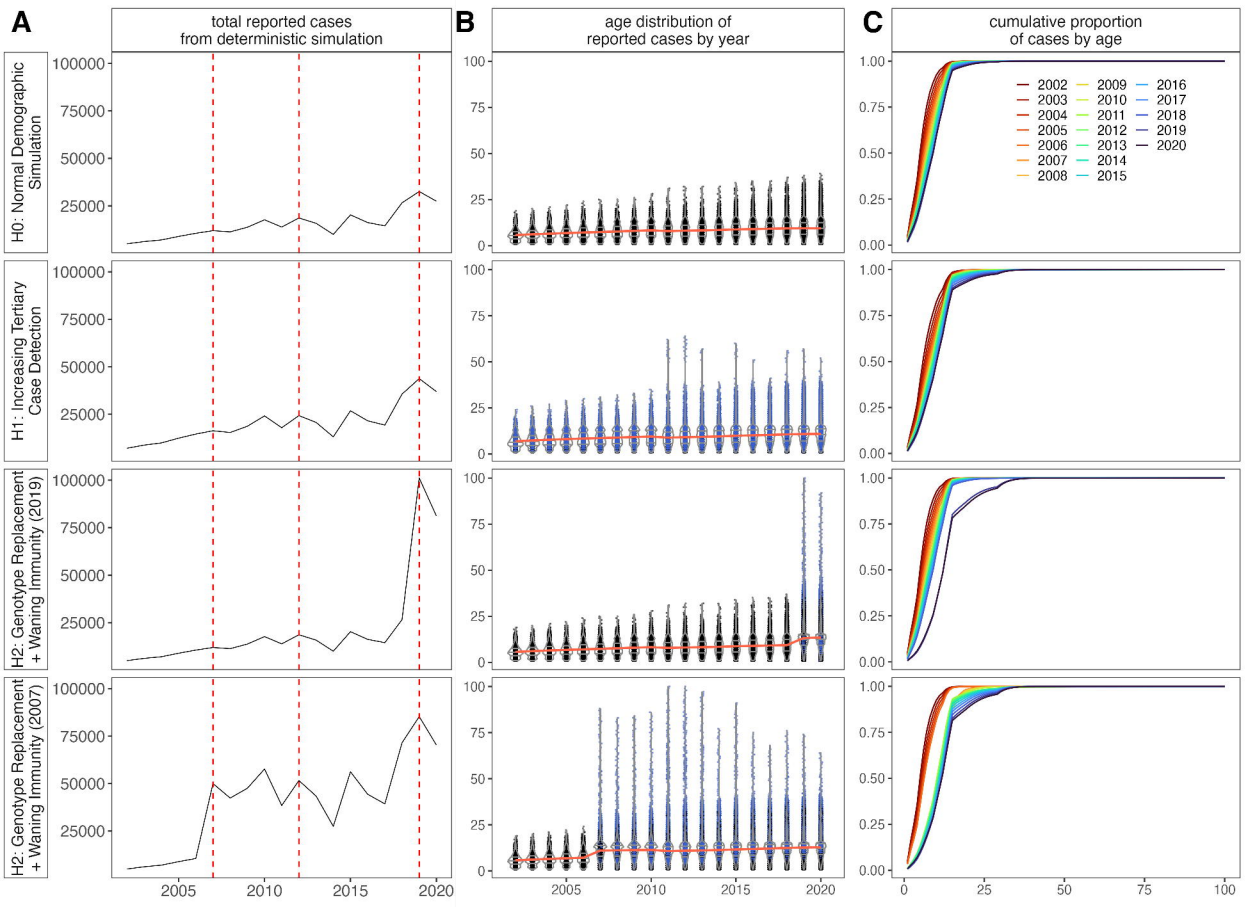
A
total reported cases
from deterministic simulation
B
age distribution of
reported cases by year
C
cumulative proportion
of cases by age
H0: Normal Demographic Simulation
H1: Increasing Tertiary Case Detection
H2: Genotype Replacement + Waning Immunity (2019)
H2: Genotype Replacement + Waning Immunity (2007)
100000
75000
50000
25000
100
75
50
25
0
1.00
0.75
0.50
0.25
0.00
2005
2010
2015
2020
0
25
50
75
100
2002
2003
2004
2005
2006
2007
2008
2009
2010
2011
2012
2013
2014
2015
2016
2017
2018
2019
2020